

**Phase Segregation and Gas Separation Properties of
Thermally Treated Copoly(ether-imide) from an Aromatic
Dianhydride, an Aromatic Diamine and Various Aliphatic
Diamines**

| | |
|-------------------------------|---|
| Journal: | <i>Industrial & Engineering Chemistry Research</i> |
| Manuscript ID: | Draft |
| Manuscript Type: | Article |
| Date Submitted by the Author: | n/a |
| Complete List of Authors: | Tena, Alberto; Universidad de Valladolid, Física Aplicada Marcos-Fernandez, Angel; Instituto de Ciencia y Tecnología de Polímeros (CSIC) Palacio, Laura; Universidad de Valladolid, Física Aplicada Cuadrado, Purificación; Universidad de Valladolid, Química Orgánica Pradanos, P.; University of Valladolid, Física Aplicada De Abajo, Javier; Instituto de Ciencia y Tecnología de Polímeros (CSIC), Macromolecular Chemistry Lozano, Angel; Instituto de Ciencia y Tecnología de Polímeros, Química Macromolecular Hernandez, Antonio; Universidad de Valladolid, Física Aplicada |
| | |

SCHOLARONE™
Manuscripts

Phase Segregation and Gas Separation Properties of Thermally Treated Copoly(ether-imide) from an Aromatic Dianhydride, an Aromatic Diamine and Various Aliphatic Diamines

Alberto Tena^{1,2}, Angel Marcos-Fernández^{1,2}, Laura Palacio^{1,3}, Purificación Cuadrado^{1,4}, Pedro Prádanos^{1,3}, Javier de Abajo^{1,2}, Angel E. Lozano^{1,2} Antonio Hernández^{*1,3}

¹SMAP UA-UVA_CSIC, Parque Científico UVA, Edificio I+D, Paseo Belén, s/n, 47071 Valladolid, Spain.

²Instituto de Ciencia y Tecnología de Polímeros, CSIC, Juan de la Cierva 3, 28006 Madrid, Spain.

³Departamento de Física Aplicada, Facultad de Ciencias, Real de Burgos s/n, 47071 Valladolid, Spain.

⁴Departamento de Química Orgánica, Facultad de Ciencias, Real de Burgos s/n, 47071 Valladolid, Spain.

Summary

Copoly(ether-imide)s formed by the reaction of an aromatic dianhydride (BPDA), an aromatic diamine (ODA) and various aliphatic diamines (PEO-2000, PPO-2000, RT-1000, pTHF-1700 and pTHF-350) has been obtained. These copolymers underwent phase segregation processes, as confirmed by SAXS, when they were thermally treated

Gas permeabilities of these materials were dependent on the phase separation. Thus, a linear relationship between gas permeability and increasing percentage, and size of the domains, of the segregated phase has been obtained. The differences in the degree of segregation have been examined for the different aliphatic diamines used in the synthesis of the copolymers.

The effect of polarity, length and structure of the chain were examined in terms of permeability for the gases O₂, N₂, CO₂ and CH₄. It has been shown that long aliphatic chains with adequate polarity and the ability to specifically interact with a certain gas give better materials.

Improved selectivities, approaching to the Robeson limit, were seen as a consequence of the thermal treatment. Also, an interesting reverse selectivity has been observed for the mixture CH₄/N₂, probably due to a combined effect of a specific interaction and an increase in solubility of CH₄ in the soft segregated portions of the copolymer.

Keywords: Copoly(ether-imide) membrane; SAXS; Phase segregation; Thermal treatment; Gas separation

*tonhg@termo.uva.es

1. Introduction

Due to environmental concerns and economic interest there is an imperative need for new materials and technologies with better efficiencies in gas separation applications [1-4]. New technologies must be found quickly in order to separate gases from diverse mixtures of gases with high selectivity and productivity. In this context, the technology of gas separation by membranes is considered a viable option. Gas separation membranes are very competitive for technological and economic reasons; they have good mechanical properties, they show excellent gas productivity (flux and ability to separate complex mixtures of gases) and they are very easy to install and maintain [5,6].

Glassy polymers show good properties as membrane materials for gas separations. In particular aromatic polyimides are well known for their excellent thermal oxidative stability, exceptional mechanical properties, along with an extraordinary ability to separate complex mixtures of gases in diverse applications [7-9]. These polymers are close to the trade-off of gas permeability versus gas selectivity obtained by Robeson in 1991 [10] for several gases. Nevertheless, they are below the new bound established in 2008 [11]. In this context, the manufacture of new polymeric materials tailored for more specific applications, with improved properties, is needed today.

A very promising means of developing new materials with improved properties consists of optimizing the structure of the polymer chains to attain high fractional free volume domains with a tailored distribution of sizes in order to increase the diffusivity and also with restrictive or selective channels communicating the interchain voids to increase the perm selectivity. Another possible approach consists of increasing the solubility by introducing moieties in the polymer with a certain chemical affinity for a gas [12,13]. The introduction of polar groups that can interact favourably with CO₂ is a very attractive idea that has brought about new materials with enhanced properties. In this regard, polymers having poly(ethylene oxide) (PEO) chains are being extensively tested because of the strong affinity of CO₂ for the oxygen of the oxyethylenic moieties [14-17]. For instance, Okamoto et al. designed a new generation of block aliphatic-aromatic copolymers with PEO units that produced materials with good mechanical properties and excellent ability to separate carbon dioxide from other gases [18-20].

In previous papers, it was demonstrated that copoly(ether-imide)s with long poly(ethylene oxide) chains of 6000 g/mol showed phase separation morphology, which can be largely improved by the use of thermal treatments [21-23]. Additionally, this thermal conditioning led to an important improvement in gas permeation properties [22].

Not many studies, to our knowledge, have analyzed the influence of the nature of the polyether segment in the gas separation properties in aliphatic-aromatic copolyimides. Hence, we have carried out a complete study of the influence of using different types of aliphatic diamines on final properties.

In a previous paper a commercial Jeffamine having a molecular weight of 2000 (PEO-2000) was combined with three aromatic diamines: p-phenylenediamine (PPD), 4,4'-diaminobiphenyl (BNZ) and 4,4'-oxydianiline (ODA). These diamines was reacted with 3,3',4,4'-biphenyltetracarboxylic dianhydride (BPDA) to form aliphatic-aromatic copolyimides. It was shown that ODA copolymers gave larger segregated domains due

1
2
3 to their limited rigidity without compromising the mechanical properties of the resulting
4 copolyimides. Thus, ODA will be used in this work as the aromatic diamine, BPDA as
5 the dianhydride, and various aliphatic diamines (PEO-2000, PPO-2000, RT-1000,
6 pTHF-1700 and pTHF-350 were employed) (see Figure 1).
7

8
9 An exhaustive study of the properties of the copolyimides (as films obtained by the
10 deposition-evaporation method) containing different aliphatic diamines, has been
11 carried out by ATR-FTIR, DSC, TGA, TMA, and SAXS after the use of different
12 thermal treatments. The corresponding permeability, solubility, diffusivity and
13 selectivity for different gases have also been studied.
14

15 **2. Experimental**

16 *2.1. Chemicals*

17
18
19 3,3',4,4'-Biphenyltetracarboxylic dianhydride (BPDA), and 4,4'-oxydianiline (ODA)
20 were purchased from Sigma-Aldrich Co. These products were purified by sublimation
21 at high vacuum just before being used. Bis(2-aminopropyl) poly(ethylene oxide), PEO-
22 2000, (Jeffamine ED-2003) with nominal molecular weight of 2000 g/mol, bis(2-
23 aminopropyl) poly(propylene oxide), PPO-2000, (Jeffamine D-2000) with nominal
24 molecular weight of 2000 g/mol, and bis(2-aminopropyl) poly(tetramethylene oxide-
25 propylene oxide) (80 % / 20 % w/w) copolymer, RT-1000, with nominal molecular
26 weight of 1000 g/mol (where $n + m = 13-15$), were kindly donated by Huntsman[®]
27 (Holland). Bis(amine) poly(tetramethylene oxide), pTHF-350 ($n=2.2$) and pTHF-1700
28 ($n= 13.5$), with two different nominal molecular weights of 350 and 1700 g/mol,
29 respectively, were a kind gift from BASF[®] The Chemical Company (Germany). All
30 amino-terminated polyethers were dried at 70°C under vacuum for 5 hours and stored in
31 a desiccator at vacuum until use. Anhydrous N-methylpyrrolidinone (NMP), used as the
32 polymerization solvent, was purchased from Sigma-Aldrich. Figure 1 shows the
33 chemical structure of the monomers.
34
35
36

37 *2.2. Synthesis of copoly(ether-imide)s*

38
39 The polymer samples were synthesized by combination of the dianhydride BPDA with
40 an aromatic amine, ODA, and an aliphatic amine (PEO-2000, PPO-2000, RT-1000,
41 pTHF-350 or pTHF-1700). The corresponding copoly(ether-imide) will be designated
42 by adding cPI before the acronym for the aliphatic portion. Thus, as an example, cPI-
43 PEO-2000 means the copolymer of BPDA, ODA and PEO-2000.
44
45

46
47 Actually, the synthesis of all the polymers shown here consisted of making a mixture of
48 4,4'-oxydianiline (ODA) (x mmol), and the aliphatic diamine (PEO-2000, PPO-2000,
49 RT-1000, pTHF-350 or pTHF-1700) (y mmol) in a weight ratio of 1:2. This mixture
50 was dissolved in anhydrous NMP (5 mmol ($x+y$)/10 mL) in a 100 mL three-necked
51 flask blanketed with nitrogen. Next, the reaction mixture was cooled to 0 °C, and under
52 mechanical stirring, a stoichiometric amount of BPDA dianhydride ($x+y$ mmol) was
53 added and stirred overnight at room temperature (see final resulting amounts in Table
54 1).
55

56
57 During this time the dianhydride completely dissolved and the solution reached high
58 viscosity.
59
60

1
2
3
4 In the case of pTHF polyethers, the material has not only primary amines, but also
5 contains some secondary amines and a minimum amount of tertiary amines. Supplier
6 gives content for the different amines of 80.1, 18.8 and 1.1% for pTHF-350 and 72.1,
7 26.5 and 1.3% for pTHF-1700 corresponding to primary, secondary and tertiary amines
8 respectively. In the synthesis calculation, the γ mmol for PTHF polyethers was
9 calculated respect to primary amines only, in order to avoid the reaction of the
10 secondary amines that would lead to chemical crosslinking. Nevertheless, the species
11 with tertiary amines are trifunctional with primary amines in the chain ends, and some
12 chemical crosslinking is unavoidable. For this reason, in the cases of pTHF-350 and
13 pTHF-1700 a certain amount of gelled material was obtained after completion of the
14 reaction. This gel was separated from the soluble fraction by filtration. The soluble part
15 of the reaction was considered as the final linear copolymer.
16
17
18
19

20 2.3. Preparation of dense films of copolyimide

21
22 The resultant viscous copolyamic acid solutions were diluted with NMP to attain an
23 appropriate viscosity for casting, filtered through a nominal #1 fritted glass funnel,
24 degassed, and cast onto levelled glass plates. The resulting films were covered with a
25 conical funnel to avoid fast evaporation of the solvent, dried at 80 °C overnight, treated
26 at 120 °C for 8 hours and finally treated at 160 °C for 6 hours in a vacuum oven.
27 Copolymer films of 40-60 μm thickness were obtained. Additional thermal treatments,
28 mentioned in the gas permeation properties section, were carried out, on those films
29 under inert atmosphere.
30

31 2.4. Characterization methods

32
33
34 Fourier transform infrared analyses with attenuated total internal reflectance (ATR-
35 FTIR) of the films were performed at room temperature using a PerkinElmer Spectrum
36 One.
37

38
39 A Thermal Analysis Q500 instrument was used for thermogravimetric analysis (TGA)
40 of the samples. Disc sections with weights between 5 and 15 mg were cut from the
41 fabricated films and tested. When running dynamic scans, this was done in Hi-
42 Resolution mode, where the heating rate is automatically adjusted in response to
43 changes in the rate of weight loss, which results in improved resolution, with an initial
44 heating rate of 10°C/min under a flux of nitrogen.
45

46
47 Differential scanning calorimetry (DSC) analyses were carried out in a Mettler Toledo
48 (DSC 822e) calorimeter equipped with a liquid nitrogen cooler. Disc samples weighting
49 5–15 mg were cut from the films and sealed in aluminium pans. In order to monitor the
50 changes in their thermal properties with thermal treatment the samples were heated with
51 the following cyclic method: from 25 °C, the sample was heated at 10 °C/min to a target
52 temperature; once reached, the sample was cooled at the maximum cooling rate
53 accessible for the instrument to -90 °C, held at this temperature for 15 min to equilibrate
54 and reheated at 10°C/min to the next target temperature. The procedure was followed
55 until the last treatment temperature was reached. In this way, in each heating run, the
56 thermal properties for the copolymers after treatment to the previously reached
57 temperature were obtained.
58
59
60

Small-Angle X-ray Scattering (SAXS) measurements were performed at the beamline BM16 at the European Synchrotron Radiation Facility (Grenoble, France). The wave length of the X-ray beam was 0.980 Å. The detector was calibrated with silver behenate ($\text{AgC}_{22}\text{H}_{43}\text{O}_2$), and distance L was calculated from the scattering vector ($q=4\pi(\sin\theta)/\lambda$, λ =wave length, 2θ =scattering angle) as

$$L = \frac{2\pi}{q} \quad (1)$$

according to Bragg's Law. Disc samples cut from films were placed in a Linkam hot stage and heated at 10°C/min while the SAXS spectra were recorded.

Thermomechanical (TMA) tests were performed in a Rheometric Scientific instrument model DMTA V. Rectangular test pieces of 3 mm width and 20 mm length were cut from films. A distance of 10 mm was set between fixation clamps. Runs were carried out from ambient temperature at 10 °C/min with a static stress of 3 MPa.

The densities (ρ) of the dense membrane films were determined using a CP225D Sartorius balance, provided with an immersion density kit, according to

$$\rho = \rho_0 \frac{W_{\text{air}}}{W_{\text{air}} - W_{\text{liq}}} \quad (2)$$

where ρ is the density of the film, W_{air} and W_{liq} are the weights of the film in the air and an auxiliary liquid [24]) and ρ_0 is the density of the auxiliary liquid (isooctane).

2.5. Gas permeation and selectivity

The permeability, P , has been determined for several gases (O_2 , N_2 , CO_2 and CH_4) by using a permeator with constant volume and variable pressure which uses the *time-lag* operation method. The measurements were carried out at 3 bar and 30 °C. The equations used and the mode of operation of equipment, as well as an outline of it has been explained in previous studies [12].

3. Results and discussion

3.1 Copoly(ether-imide)s imidization

Poly(ethylene oxide), poly(propylene oxide) and poly(tetramethylene oxide) chains are prone to oxidation [25] and therefore, a great care was taken to carry out the imidization process. The films were heated at 160 °C for 6 h. By thermogravimetric analysis it was found that the solvent was practically removed by this heat treatment. It should be noted that all the copolymers were found to be insoluble in DMAc (dimethylacetamide), NMP, Hexane, Toluene, THF (tetrahydrofuran), CH_2Cl_2 (dichloromethane) after this process.

Infrared spectra were recorded for these membranes (heated at 160 °C for 6 h) to check for the progress of imidization. As already seen for similar copolyimides [22], bands centered around 3257, 2500 and 1657 cm^{-1} found in the casted copolyamic acid strongly decrease or disappear with the thermal treatment, and bands at approximately 1774,

1713, 1372 and 738 cm^{-1} increase or appear with the progress on the imidization reaction, the last one being identificative of BPDA derived imides (see figure 2). The peaks appearing around 2800 cm^{-1} are due to the aliphatic polyether segments.

For similar copoly(ether-imide)s to the ones presented here, Hangzheng et al. [26], used IR spectra to prove the imidization at 200 °C. Even though the complete imidization of our copolyimides at temperature as low as 160 °C is actually remarkable, we must mention that this full imidization at relatively low temperatures had already been found by us for copoly(ether-imide)s based on PEO segments [22,27]. Also, two works of Okamoto et al., studying similar copoly(ether-imide)s to the ones presented here, stated that a thermal treatment at 170 °C completely imidize the precursor poly(amic acid)s to polyimides [18,19] although they did not show any IR spectra to prove the imidization state of the copolymers.

3.2 Thermal stability

Thermogravimetric analysis was performed to evaluate the thermal stability of the copolymers. Dynamic runs using the HiREs mode, in a nitrogen atmosphere, showed a weight loss pattern for all the samples after being treated at 160 °C during 6 hours. The resulting thermograms are shown in Figure 3.

The behaviour was similar for the different samples. The initial mass loss (close to 2% weight from ambient temperature to 100 °C) can be attributed to the absorbed water in the sample. The second step is thought to be due to the loss of the aliphatic part included in the copolymer composition. In all the cases, the temperature of maximum rate of weight loss was above 300 °C, but clearly higher for the copolymers containing tetramethylene oxide units (385, 407 and 382 °C for cPI-RT-1000, cPI-pTHF-350 and cPI-pTHF-1700 respectively) respect to the polymers containing ethylene oxide (363 °C for cPI-PEO-2000) or propylene oxide (345 °C for cPI-PPO-2000) units, showing the higher thermal stability of the former. After this degradation, a third step was attributed to the generalized degradation of the residual aromatic part. For all copolymers, the residual carbon content at 800 °C was 32-34%.

The differences between the mass losses in the second step for the different copolyimides studied are due to different percentages of polyether blocks in the polymers as evidenced by the good agreement between the experimental loss and what should be expected according to mass balances. This is shown in Figure 4. Note, however, that cPI-pTHF-350, that has the highest temperature of degradation for this step, is totally out of line with this correlation. In this case, because of the low molecular weight of the polyether chains, the aromatic polyimide segments are shorter than for the other copolymers and degrade at lower temperature producing a merging of the degradation of the aliphatic and remaining aromatic portions, that cannot be clearly separated as for the other copolymers.

Thus, TGA analyses confirmed that the aliphatic-chain thermal stability is much lower than the thermal stability of the aromatic polyimide segments, and therefore a selective degradation of this part can be performed in these copolymers with long polyether chains, as has been reported for other similar polymers [28, 29].

3.3 Calorimetric studies

The samples were heated in a DSC instrument with a cyclic method in order to monitor the changes in the thermal properties of the films with the thermal treatment. When the polyether moiety is able to crystallize, the melting enthalpy can be used to evaluate the phase separation of the segments [22]. For the copolymers prepared in this work, cPI-PEO-2000 had a crystallinity lower than 2 % after thermal treatments, while cPI-PPO-2000, cPI-RT1000, cPI-pTHF-350 and cPI-pTHF-1700 were totally amorphous. No transition related to the aromatic polyimide hard segments was detected by DSC in any case.

In figure 5 we can see the changes in T_g for the different treatment temperatures. Only minor changes are seen that could be due to the increase in the proportion and size of the segregated domains along with the release of the remaining traces of solvent. The T_g for the copolymers with approximately 2000 g/mol follows the trend of the corresponding homopolymers: pTHF < PPO < PEO. Copolymer cPI-RT1000, with shorter chains has a higher T_g , and for copolymer cPI-pTHF-350, chains are so short that phases are significantly mixed and T_g reaches a value well above room temperature. Thus, from these results, it can be asserted that for all the copolymers studied, at the temperature of measurement of permeability the polyether segments were totally amorphous and well above their T_g except for copolymer cPI-pTHF-350.

3.4 Thermomechanical analysis

Thermomechanical analysis was also carried out in order to detect the glass transition temperature of the aromatic polyimide hard segments, which could not be detected by DSC. It was assumed that a good estimation of T_g corresponds to the temperature when strain is 10 times that of the sample at 100 °C [22]. This criterion could be accepted at least for comparative purposes. The thus-obtained results are shown in Figure 6.

The corresponding results for T_g are shown as a function of the copolymer density in Figure 7. The data on permeability and density for the BPDA-ODA homopolymer are taken from literature [30]. Note that there is a clear increase of the T_g for the aromatic portion of the copolymers with increasing copolymer densities for polyethers of relatively long chains. This is nevertheless clearly not the case for cPI-pTHF-350. This anomalous fact could be due to the very short length of the pTHF-350 chains and their close interaction with the aromatic chains in the copolymer leading to a very significant mixture of the segments, as already seen by DSC.

For all the copolymers, the T_g of the aromatic polyimide is well above ambient temperature, although lower than the corresponding T_g for a pure aromatic polyimide homopolymer, due to the much lower polymerization degree and, consequently, lower length of the aromatic polyimide segments in the copolymer as compared to the corresponding homopolymer [22].

All samples have the same aromatic part, so that the observed differences should only be due to the different mode of packaging of the aliphatic part in the final polymer structure. For this reason, a better segregation in phases would increase the T_g of the aromatic portion. Under this assumption, it could be observed that the cPI-PEO-2000 sample showed the highest T_g value, followed by the cPI-RT-1000 and PPO-2000 ones.

The lowest T_g values were obtained for samples with pTHF where phase segregation is likely to be poor.

3.5. Small-angle X-ray scattering

Two parameters can be calculated from these scattering curves: the relative invariant, Q', as the integral below the curve Iq² vs. q, which is related to the extent of the phase separation; and the maximum on the scattering curve, q_{max}, related to the size scale of the separated phases, calculated also from the curve Iq² vs. q. The equations used and the mode of operation of the equipment, as well as an outline of it has been explained in previous studies [27].

Actually, the length scale, L, of the phase separation can be accurately evaluated from the curve Iq² vs. q only for lamellar morphologies, [31]. Nevertheless, our aim here is to compare L for some copolymers that are similar in structure. Thus, this procedure will be followed attending to its simplicity. Essentially, to eliminate the influence of the different film thicknesses and electronic density, the relative increment of both parameters is defined as,

$$\Delta Q' = \frac{Q'(T) - Q'(\text{baseline at } T)}{Q'(\text{baseline at } T)} \quad (3)$$

$$\Delta L = \frac{L(T) - L(\text{baseline at } T)}{L(\text{baseline at } T)} \quad (4)$$

The obtained results for ΔQ' and ΔL, are represented in Figure 8 and 9 for the copoly(ether-imides) studied. In the curves shown in these figures, for the sample treated at 160 °C, there is a change in both the relative invariant and the characteristic length of the segregated phases, that appears in the range from 170 to 300 °C (the increase is continued until the end of the temperature range tested). After heating at 300 °C, the final length scale for the copolymers lied in between 10 and 13 nm, which is smaller than the values for similar copolymers with longer polyether chains [22].

3.6. Mechanical properties

To complete the study on the physical properties of these copoly(ether imide)s, mechanical properties were measured in tensile mode for copolymer films treated at 160 °C for 6 hours. The obtained results are shown in Table 2.

It is worth noting that all the copolymers showed reasonably good mechanical properties. Copolymer cPI-pTHF-1700 had better mechanical properties than copolymers with similar polyether length (cPI-PEO-2000 and cPI-PPO-2000). This is somewhat expected given that for other copolymers based on these polyethers such as polyurethanes, it is well known that poly(tetramethylene oxide) polyethers produce stronger materials than poly(propylene oxide) or poly(ethylene oxide) polyethers. In the case of copolymer cPI-pTHF-350, because of the extensive mixing of the segments, the copolymer is much more rigid than the other ones as it can be deduced for the value of the modulus, and the properties lie in between the value of the copolymer with longer polyether segments and the values for the pure aromatic polyimide BPDA-ODA [22].

3.7. Gas permeation and selectivity

Figure 10 presents the permeability coefficients for the O₂, N₂, CH₄, and CO₂ gases in films of cPI-PEO-2000 as a function of the temperature of treatment. It could be observed that all the synthesized copolyimides showed similar trends. Permeability increased with the temperature of treatment of the copolymer, following the sequence:

$$P(\text{CO}_2) > P(\text{CH}_4) \sim P(\text{O}_2) > P(\text{N}_2)$$

This is the order of decrease of the critical temperature of the penetrant gas (*i.e.*, decreasing penetrant condensability). For these types of compounds, the diffusion coefficient is only a weak function of the penetrant size, because the polymer size-sieving ability is poor, [32]. In our case, as the penetrant size increased, the solubility coefficient increased more strongly than the diffusion coefficient decreased, which means that larger, more condensable penetrants are more permeable than smaller ones [33]. Therefore, in these materials the relative permeability of each penetrant is largely determined by its solubility.

Figure 11 illustrates the effect of the thermal treatment on the CO₂ permeability. The tendency was quite similar for all the copolymers, with the exception of the sample pTHF-350, which showed very low permeability differences. The increase in permeability was always higher for treatment temperatures over 250 °C, when most of the possible residual solvent is released and the improvement in the phase separation is higher. In the case of films from cPI-PPO-2000, the increase in permeability was especially intense.

For all the copolymers, the selectivity versus diffusivity and the solubility-selectivity versus the diffusivity-selectivity for the different pairs of gases and the temperature treatments are shown in Figures 12-16. For the CH₄/N₂ pair (Figure 15) given that no bound has been proposed yet, a bound is drawn on the basis of some good results from literature [34-39].

Note that for all the gas pairs the permeability of cPI-pTHF-350 was very low corresponding to its very low phase segregation as has been shown in Figures 8 and 9. Regarding the CO₂/N₂ and CO₂/CH₄ gas pairs, cPI-PEO-2000 presented the highest selectivity while the highest permeability appeared for cPI-PPO 2000. Note that both $\Delta Q'$ and ΔL increased strongly with thermal treatment for cPI-PPO-2000. Thus, it seems that the extension of segregation ($\Delta Q'$) and the mean size of the segregated domains (ΔL) increased the permeability of CO₂ and the rest of the gases studied. The selectivity for all the pairs including CO₂ was especially high for cPI-PEO-2000 probably due to specific interactions and to the big surface of its segregated domains, as seen in Figure 8, although neither this dimension nor the invariant (see Figure 9) increased notably with the treatment temperature.

Since the copolyimides studied here can be assumed as consisting of a non-segregated (continuous) aromatic polyimide phase and a soft segregated (disperse) aliphatic phase, the effective permeability of each copolyimide may be predicted by the Maxwell equation as shown below [40]:

$$P_{\text{eff}} = P_C \left[\frac{P_D + 2P_C - 2\phi_D(P_C - P_D)}{P_D + 2P_C + 2\phi_D(P_C - P_D)} \right] \quad (5)$$

P_{eff} is the effective permeability, P_C and P_D are the permeability of the continuous phase and of the dispersed phase, respectively, and ϕ_D is the volume fraction of the dispersed phase in the block copolymer. The permeability of CO_2 for a pure PEO is known to be 143 Barrer in the amorphous state [41] and it is taken as P_D while the permeability of the copolyimide treated at 120 °C (when segregation has not advanced appreciably, according to Figures 8 and 9) is assumed for P_C . Thus, this method could be used in order to attain ϕ_D (i.e. the fraction of segregated PEO) in cPI-PEO-2000. Because the permeability of pure aliphatic constituents of the other copolyimides studied in this paper is not accessible, this method has been used only for the cPI-PEO-2000 polymer.

The thus-obtained volume fractions of segregated PEO (for CO_2) are shown as a function of the temperature of treatment in Figure 17. The maximum volume fractions evaluated either from the initial mass balance used to make the polymers or from the TGA results, taking into account the densities of pure PEO and BPDA-ODA homopolymer, are shown in Figure 17. It is clear that the treatment temperature was so efficient in segregating the PEO moieties that after treatment of the membranes at 250 °C almost all the available PEO was segregated.

It is worth noting that the Maxwell equation is accurate only when the components in the medium are mutually independent [42]. Therefore, the fractions shown in Figure 17 could be only an estimation if a non-negligible interaction between soft and hard segments in the copolymer was supposed to exist. Obviously, the existence of the simultaneous imidization processes could also lead to erroneous evaluations of fractions. All these possible sources of error do not put into risk the conclusion on the high efficiency of thermal treatment to cause almost total segregation of the aliphatic components of the copolymer. Moreover if one assumes that the maximum segregation corresponds to the maximum PEO contained in the copolymer, the percentage of segregation already reached at 120 °C is less than a 10 % as can be seen in Figure 17.

In terms of permselectivity (see Figures 12-16) the separation performances when the gases involved in the mixtures have different polarity (CO_2/N_2 and CO_2/CH_4) follow the sequence of polarities of the aliphatic portion of the copolymers: PEO-2000 > PPO-2000 > RT-1000 /pTHF-1700. In the selectivity versus permeability plots, the copolymer with better performances (closer to the corresponding Robeson's bound) is identified by a dotted line. Again, the permselectivity for pTHF-350 was very low due to the lack of phase segregation. When polarities are similar – with similar (O_2/N_2) or quite different (CH_4/N_2) sizes – the copolymer sequence follows the evolution of $\Delta Q'$ or ΔL (see Figures 8 and 9).

In the case of the CH_4/N_2 gas pair, the cPI-PPO-2000 copolymer showed the highest permeability along with better selectivity. This extra selectivity that can even overcome the high solubility of the condensable gases that presents cPI-PEO-2000 can only be due to the presence of CH_3 - groups contained within the PPO-2000 chain because this group is able to interact in a favorable way with CH_4 . The cPI-pTHF-1700 presented the

1
2
3 second lowest permeability and selectivity (once more cPI-pTHF-350 was the
4 copolymer that gave the worst gas productivity). cPI-RT-1000 (the copolymer with
5 poly(tetramethylene oxide) and poly(propylene oxide) in its structure) gave
6 permeability and selectivity values in between those shown by cPI-PPO-2000 and cPI-
7 PEO-2000.
8

9
10 On the other hand, the balance of the selectivity by diffusivity versus the selectivity by
11 solubility proved that for all the couples of gases studied in this paper the selectivity
12 was controlled mainly by the solubility term except for the O₂/N₂ pair where the
13 diffusive selectivity played a mayor role. At this point, it is interesting to remark that the
14 use of higher temperature during the thermal treatment increased the balance between
15 the solubility and the diffusive terms of selectivity.
16

17 18 **4. Conclusions**

19
20 Copoly(ether-imide)s have been synthesized by the reaction between an aromatic
21 dianhydride (BPDA), an aromatic diamine (ODA) and various diamine terminated
22 aliphatic polyether (PEO-2000, PPO-2000, RT-1000, pTHF-1700 and pTHF-350.
23

24
25 FTIR showed that full imidization is almost achieved for all copolymers after a thermal
26 treatment at 160 °C, well below the temperature needed to imidize fully aromatic
27 polyimides. Based on TGA data, these copolymers proved to be stable under inert
28 atmosphere up to around 300 °C. The TGA plots have determined that, it is possible to
29 make a selective degradation of the polyether segments except for the copolymer cPI-
30 pTHF-350, with very short polyether chains. Mechanical properties for these
31 copolymers were good enough to be applied in gas separation applications.
32

33
34 DSC, TMA and SAXS experiments proved the existence of a phase separated
35 morphology in these copolymers that improved when they were thermally treated at
36 increasing temperatures below the temperature of the onset of decomposition. The phase
37 segregation consisted of a polyether phase (completely amorphous at ambient
38 temperature) and an aromatic polyimide phase with a T_g well above ambient
39 temperature, except for cPI-pTHF-350 that had a very extensive mixing of segments.
40

41
42 For high treatment temperatures, the normalized or relative degree of segregation of the
43 phases followed the sequence pTHF-1700 > PPO-2000 > PEO-2000 > RT-1000 >
44 pTHF-350, whereas the relative increment of size scale of the segregated domains
45 followed the progression PPO-2000 > pTHF-1700 > RT-1000 / PEO-2000 > pTHF-350.
46 As a consequence of the thermal treatment, the properties of the copolymers changed as
47 their degree of segregation proceeded. Initially, at intermediate treatment temperatures,
48 the release of the remaining solvent in the imidized copolymers produced a fast
49 improvement in the phase separation, and treatments at higher temperatures (up to the
50 degradation temperature) produced further improvement.
51

52
53 After phase segregation, all of the samples show increasing selectivity for the studied
54 pairs of gases. This fact was due to the increasing percentage and size of the domains of
55 the segregated phases that determined the extra permeability and selectivity shown for
56 the films after higher treatment temperatures.
57
58
59
60

1
2
3 In terms of permselectivity the gas performances when the gases had different polar
4 nature, followed the sequence of polarities of the aliphatic part of the copolymers.
5 Finally, when polarities were similar the gas productivity sequence followed the trend
6 of the extent of segregation and the size of the segregated domains that were quite
7 similar. For the case of the CH₄/N₂ separation, an interesting reverse selectivity appeared
8 probably due to the existence of interactions between CH₄ and the soft segregated
9 aliphatic moieties of the copolymers.
10

11
12
13 The main results pointed to in this work were: the effect of the structure and the
14 percentage of the aliphatic diamines used to make the copolymer, the temperature of
15 treatment and also the possibility of adapting polarity and chemical nature of the
16 aliphatic chains which open a wide range of options for the optimization of these
17 aromatic-aliphatic copolyimides to tailor their functionality to different applications in
18 industrial processes.
19

20 21 22 **5. Acknowledgements**

23
24 We are indebted to the Spanish Junta de Castilla-León for their financing of this work
25 through the GR-18 Excellence Group Action and to the Spanish Ministry of Science and
26 Innovation (MICINN) for the economic support of this work (MAT2008-00619/MAT,
27 CIT-420000-2009-32 and MAT2010-20668/MAT). We also acknowledge financial
28 support from the programme CONSOLIDER, project Multicat.
29

30
31 Authors are thankful for the access to the beamline BM16 at the European Synchrotron
32 Radiation Facility (ESRF) in Grenoble (France). We are grateful to Dr. Ana Labrador
33 and Dr. François Fauth for their help at BM16 station at the ESRF. The help provided
34 by Sara Rodríguez in measuring gas properties is greatly appreciated. Advice from Dr.
35 Jack Preston is greatly appreciated. A. Tena thanks CSIC for the predoctoral JAE
36 fellowship received to carry out this work.
37

38 39 **6. References**

- 40
41 1. Robeson, L.M. Polymer membranes for gas separation. *Curr. Opin. Solid State*
42 *Mater. Sci.* **1999**, *4*, 549–552.
43 2. Pandey, P.; Chauhan, R.S. Membranes for gas separation. *Prog. Polym. Sci.* **2001**, *26*,
44 853-893.
45 3. Koros, W.J. Gas separation membranes: Need for combined materials science and
46 processing approaches. *Macromol. Symp.* **2002**, *188*, 13–22.
47 4. Ulbricht, M. Advanced functional polymer membranes, *Polymer.* **2006**, *47*, 2217–
48 2262.
49 5. Baker, R.W. Future directions of membrane gas separation technology. *Ind. Eng.*
50 *Chem. Res.* **2002**, *41*, 1393–1411.
51 6. Lin, H.; Freeman, B.D. Materials selection guidelines for membranes that remove
52 CO₂ from gas mixtures. *J. Mol. Struct.* **2005**, *739*, 57–74.
53 7. Bessonov, M.T.; Koton, M.M.; Kudryavtsev, V.V.; Laius, L.A. Polyimides:
54 Thermally Stable Polymers; Consultants Bureau, New York, 1987.
55 8. Wilson, D.; Stenzenberger, H.D.; Hergenrother, P.M. Polyimides; Blackie: Glasgow,
56 1990.
57
58
59
60

- 1
- 2
- 3 9. Ghosh, M.K.; Mittal, K.L. Polyimides: Fundamentals and Applications; Marcel
- 4 Dekker: New York, 1996.
- 5 10. Robeson, L.M. Correlation of separation factor versus permeability for polymeric
- 6 membranes. *J. Membr. Sci.* **1991**, *62*, 165-185.
- 7 11. Robeson, L.M. The upper bound revisited. *J. Membr. Sci.* **2008**, *320*, 390-400.
- 8 12. Tena, A.; Fernández, L.; Sánchez, M.; Palacio, L.; Lozano, A.E.; Hernández, A.;
- 9 Prádanos, P. Mixed matrix membranes of 6FDA-6FpDA with surface functionalized
- 10 gamma-alumina particles. An analysis of the improvement of permselectivity for
- 11 several gas pairs. *Chem. Eng. Sci.* **2010**, *65* (6), 2227-2235.
- 12 13. Ghosal, K.; Chen, R.T.; Freeman, B.D.; Daly, W.H.; Negulescu, I.I. Effects of basic
- 13 substituents on gas sorption and permeation in polysulfone. *Macromolecules.* **1996**, *29*,
- 14 4360-4369.
- 15 14. Kawakami, M.; Iwanaga, H.; Hara, Y.; Iwamoto, M.; Kagawa, S. J. Gas
- 16 permeabilities of cellulose nitrate/poly(ethylene glycol) blend membranes. *J. Appl.*
- 17 *Polym. Sci.* **1982**, *27*, 2387-2393.
- 18 15. Li, J.; Nagai, K.; Nakagawa, T.; Wang, S. Preparation of Polyethyleneglycol (PEG)
- 19 and Cellulose Acetate (CA) Blend Membranes and Their Gas Permeabilities. *J. Appl.*
- 20 *Polym. Sci.* **1995**, *58*, 1455-1463.
- 21 16. Lin, H.; van Wagner, E.; Swinnea, J.S.; Freeman, B.D.; Pas, S.J.; Hill, A.J.;
- 22 Kalakkunnath, S.; Kalika, D.S. Transport and structural characteristics of crosslinked
- 23 poly(ethylene oxide) rubbers. *J. Membr. Sci.* **2006**, *276*(1-2), 145-161.
- 24 17. Bondar, V.I.; Freeman, B.D.; Pinnau, I. Gas transport properties of poly(ether-b-
- 25 amide) segmented block copolymers. *J. Polym. Sci. Part B: Polym. Phys.* **2000**, *38* (15),
- 26 2051-2062.
- 27 18. Okamoto, K.; Umeo, N.; Okamoto, S.; Tanaka, K.; Kita, H. Selective permeation of
- 28 carbon dioxide over nitrogen through polyethyleneoxide-containing polyimide
- 29 membranes. *Chem. Lett.* **1993**, *5*, 225-228.
- 30 19. Okamoto, K.; Fujii, M.; Okamoto, S.; Suzuki, H.; Tanaka, K.; Kita, H. Gas
- 31 permeation properties of poly(ether imide) segmented copolymers. *Macromolecules.*
- 32 **1995**, *28*, 6950-6956.
- 33 20. Yoshino, M.; Ito, K.; Kita, H.; Okamoto, K. Effects of hard-segment polymers on
- 34 CO₂/N₂ gas separation properties of poly(ethylene oxide)-segmented copolymers. *J.*
- 35 *Polym. Sci. Part B: Polym. Phys.* **2000**, *38*, 1707-1715.
- 36 21. Muñoz, D.M.; Maya, E.M.; de Abajo, J.; de la Campa, J.G.; Lozano, A.E. Thermal
- 37 treatment of poly(ethylene oxide)-segmented copolyimide based membranes: An
- 38 effective way to improve the gas separation properties. *J. Memb. Sci.* **2008**, *323*, 53-59.
- 39 22. Marcos-Fernandez, A.; Tena, A.; Lozano, A.E.; de la Campa, J.G.; de Abajo, J.;
- 40 Palacio, L.; Prádanos, P.; Hernández, A. Physical properties of films made of
- 41 copy(ether-imide) with long poly(ethylene oxide) segments. *Eur. Polym. J.* **2010**, *46*,
- 42 2352-2374.
- 43 23. Maya, E.M.; Muñoz, D.M.; Lozano, A.E.; de Abajo, J.; de la Campa, J.G. Fluorenyl
- 44 cardo copolyimides containing poly(ethylene oxide) segments: synthesis,
- 45 characterization, and evaluation of properties. *J. Polym. Sci. Part A: Polym. Chem.*
- 46 **2008**, *46*, 8170-8178.
- 47 24. Brandrup, J.; Immergut E.H.; Grulke, E.A. Polymer handbook (4th ed.); John Wiley
- 48 & Sons Inc: New York 1999.
- 49 25. Scheirs, J.; Bigger, S.W.; Delatycki, O. Characterizing the solid-state thermal
- 50 oxidation of poly(ethylene oxide) powder. *Polymer.* **1991**, *32*, 2014-2019.
- 51
- 52
- 53
- 54
- 55
- 56
- 57
- 58
- 59
- 60

- 1
2
3 26. Hangzheng, C.; Youchang, X.; Tai-Shung, C. Synthesis and characterization of poly
4 (ethylene oxide) containing copolyimides for hydrogen purification. *Polymer*. **2010**, *51*,
5 4077-4086.
- 6 27. Tena, A.; Marcos-Fernández, A.; Lozano, A. E.; de la Campa, J. G.; de Abajo, J.;
7 Palacio, L.; Prádanos, P.; Hernández, A. Thermally treated copoly(ether-imide)s made
8 from BPDA and aliphatic plus aromatic diamines. Dependence of gas separation
9 properties on the aromatic diamine. *J. Memb. Sci.* **2012**, *387-388*, 54-65.
- 10 28. Hedrick J.L.; Carter K.R.; Cha H.J.; Hawker C.J.; DiPietro R.A.; Labadie J.W.;
11 Miller R.D.; Russell T.P.; Sanchez M.I.; Volksen W.; Yoon D.Y.; Mecerreyes D. High-
12 temperature polyimide nanofoams for microelectronic applications, Reactive &
13 Functional. *Polymer*. **1996**, *30*, 43-53.
- 14 29. Hendrich J.L.; Charlier Y.; DiPietro R.; Jayaraman S.; McGrath J.E. High Tg
15 Polyimide Nanofoams Derived from Pyromellitic Dianhydride and 1,1-Bis(4-
16 aminophenyl)-1-phenyl-2,2,2-trifluoroethane, *J. Polym. Sci. Part A: Polym. Chem.*
17 **1996**, *34*, 2867-2877.
- 18 30. Zhang, J.; Lu, J.; Liu, W.; Xue, Q. Thin Solid Films. **1999**, *340*, 106-109.
- 19 31. Baltá-Calleja, F.S.; Vonk, C.G. X-ray scattering of synthetic polymers. Elsevier:
20 Amsterdam, 1989.
- 21 32. Reid, R. C.; Prausnitz, J. M.; Poling, B. E. The Properties of Gases and Liquids.
22 McGraw Hill: New York, 1987.
- 23 33. Recio, R.; Lozano, A. E. ; Pradanos, P.; Marcos, A.; Tejerina, F.; Hernandez, A.
24 Effect of fractional free volume and Tg on gas separation through membranes made
25 with different glassy polymers. *J. Appl. Polym. Sci.* **2008**, *107*, 1039-1046.
- 26 34. Richards, J. J.; Danquah, M. K.; Kalakkunnath, S.; Kalika, D. S.; Kusuma, V.A.;
27 Matteucci, S.T.; Freeman, B. D. Relation between structure and gas transport properties
28 of polyethylene oxide networks based on crosslinked bisphenol A ethoxylate diacrylate.
29 *Chem. Eng. Sci.* **2009**, *64(22)*, 4707-4718.
- 30 35. Teo, L. S.; Chen, C.Y.; Kuo, J. F. The gas transport properties of amine-containing
31 polyurethane and poly(urethane-urea) membranes. *J. Membr. Sci.* **1998**, *141*, 91-99.
- 32 36. Budd, P.M.; Msayib, K.J.; Tattershall, C.E.; Ghanem, B.S.; Reynolds, K.J.;
33 McKeown, N.B.; Fritsch, D. Gas separation membranes from polymers of intrinsic
34 microporosity. *J. Membr. Sci.* **2005**, *251*, 263.
- 35 37. Toy, L.G.; Nagai, K.; Freeman, B.D.; Pinnau, I.; He, Z.; Masuda, T.; Teraguchi, M.;
36 Yampolskii, Y.P. Pure-gas and vapor permeation and sorption properties of poly[1-
37 phenyl-2-[p-(trimethylsilyl)phenyl]acetylene] (PTMSDPA). *Macromolecules*. **2000**, *33*,
38 2516-2524.
- 39 38. Merkel, T.C.; Bondar, V.; Nagai, K.; Freeman, B.D. Sorption and transport of
40 hydrocarbon and perfluorocarbon gases in poly(1-trimethylsilyl-1-propyne). *J. Polym.*
41 *Sci. Part B: Polym. Phys.* **2000**, *38*, 273-296.
- 42 39. Nagai, K.; Higuchi, A.; Nakagawa, T. Gas permeability and stability of poly(1-
43 trimethylsilyl-1-propyne-co-1-phenyl-1-propyne) membranes. *J. Polym. Sci. Part B:*
44 *Polym. Phys.* **1995**, *33*, 289-298.
- 45 40. Maxwell J. C. A treatise on electricity and magnetism. Vol. 1. London MacMillan
46 Publ.: London, UK, 1873.
- 47 41. Lin, H.; Freeman, B.D. Gas solubility, diffusivity and permeability in poly(ethylene
48 oxide). *J. Membr. Sci.* **2004**, *239*, 105-117.
- 49 42. Mi, Y.; Hirose, T. Molecular design of high-performance polyimide membranes for
50 gas separations. *J Polym Res.* **1996**, *3*, 11-9.
- 51
52
53
54
55
56
57
58
59
60

Caption of Figures

Figure 1.- Chemical structure of the monomers used in this work.

Figure 2.- ATR-FTIR spectra of copoly(ether-imide)s .

Figure 3.- TGA curves in dynamic conditions of copolymers having different aliphatic diamines.

Figure 4.- Aliphatic mass losses obtained from TGA versus the corresponding mass proportions according to the manufacture procedure.

Figure 5.- Figure 5.- a) Tg of the aliphatic part of copolymers as a function of the thermal treatment. For the sake of readability, Tg of the aliphatic part of cpI-THF-350 is shown in Figure 5(b).

Figure 6.- TMA curves of copolyimides. Crosses correspond to the T_g for the aromatic segment. Polymer films were treated at 160 °C.

Figure 7.- T_g of the aromatic parts of copolymers (as shown in Figure 6) versus the density of these copolymers. Density and Tg for BPDA-ODA homopolymer are shown in the graph. Polymer films were treated at 160 °C.

Figure 8.- ΔL of copolymers as a function of treatment temperature. The characteristic length for the treatment at 160 °C is shown in the legend. Polymer films were treated at 160 °C.

Figure 9.- ΔQ' of copolymers as a function of temperature. Polymer films were treated at 160 °C.

Figure 10.- Permeability of the different gases studied as a function of the temperature of treatment for cPI-PEO-2000 copolymer.

Figure 11.- Permeability of CO₂ for the different copolyimides as a function of the temperature of treatment.

Figure 12.- Robeson plot of copolymers for the O₂/N₂ gas pair. The insert shows the corresponding solubility and diffusivity selectivities.

Figure 13.- Robeson plot of copolymers for the CO₂/N₂ gas pair. The insert shows the corresponding solubility and diffusivity selectivities.

Figure 14.- Robeson plot of copolymers for the CO₂/CH₄ gas pair. The insert shows the corresponding solubility and diffusivity selectivities.

Figure 15.- Robeson plot of copolymers for the CH₄/N₂ gas pair.

Figure 16.- Solubility and diffusivity selectivities of copolymers for the CH₄/N₂ gas pair.

Figure 17.- Volume fraction of phase segregated PEO for cPI-PEO-2000 as a function of the treatment temperature.

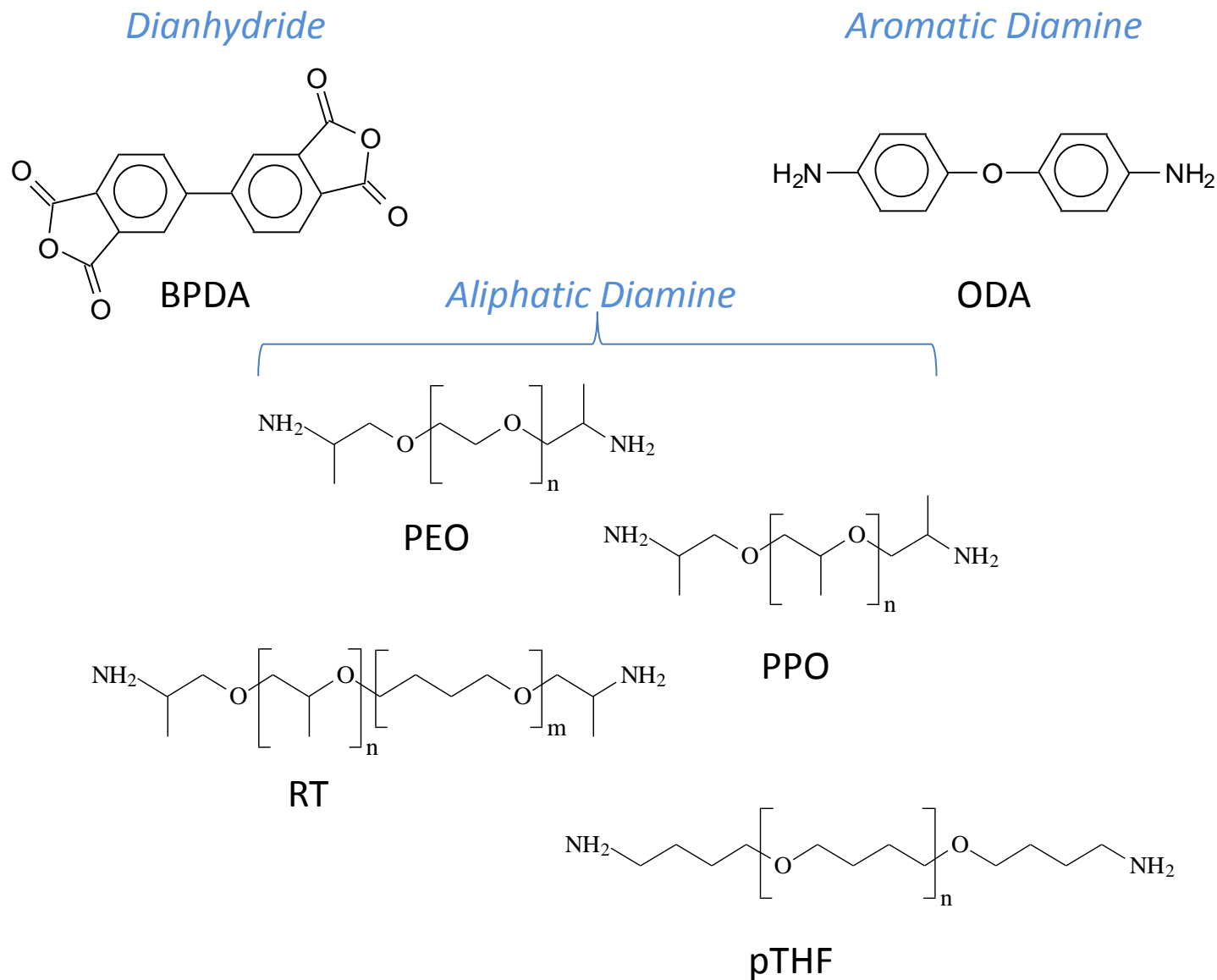
Tables

| Polymer | ODA (mmol) | Aliphatic Diamine (mmol) | BPDA (mmol) | Polyether content (% w/w) |
|---------------|------------|--------------------------|-------------|---------------------------|
| cPI-PEO-2000 | 4.99 | 1.03 | 6.02 | 43.7% |
| cPI-PPO-2000 | 5.04 | 1.04 | 6.08 | 43.8% |
| cPI-RT-1000 | 3.94 | 1.58 | 5.52 | 41.7% |
| cPI-pTHF-350 | 2.0 | 3.09 | 5.79 | 34.7% |
| cPI-pTHF-1700 | 4.54 | 1.06 | 5.61 | 43.6% |

Table 1.- Aliphatic and aromatic content of the synthesized copoly(ether-imide)s

| PROPERTY | cPI-PEO-2000 | cPI-PPO-2000 | cPI-RT-1000 | cPI-pTHF-1700 | cPI-pTHF-350 |
|----------------------|--------------|--------------|-------------|---------------|--------------|
| Maximum stress (MPa) | 22.1±1.7 | 13.5±1.9 | 18.7±1.4 | 44.4±3.4 | 75.3±2.0 |
| Strain (%) | 115±5.3 | 13.2±1.8 | 33.5±2.1 | 219±10.2 | 9.7±1.1 |
| Modulus (GPa) | 0.38±0.04 | 0.40±0.06 | 0.36±0.02 | 0.53±0.08 | 1.68±0.02 |

Table 2. Mechanical properties of copoly(ether-imide).



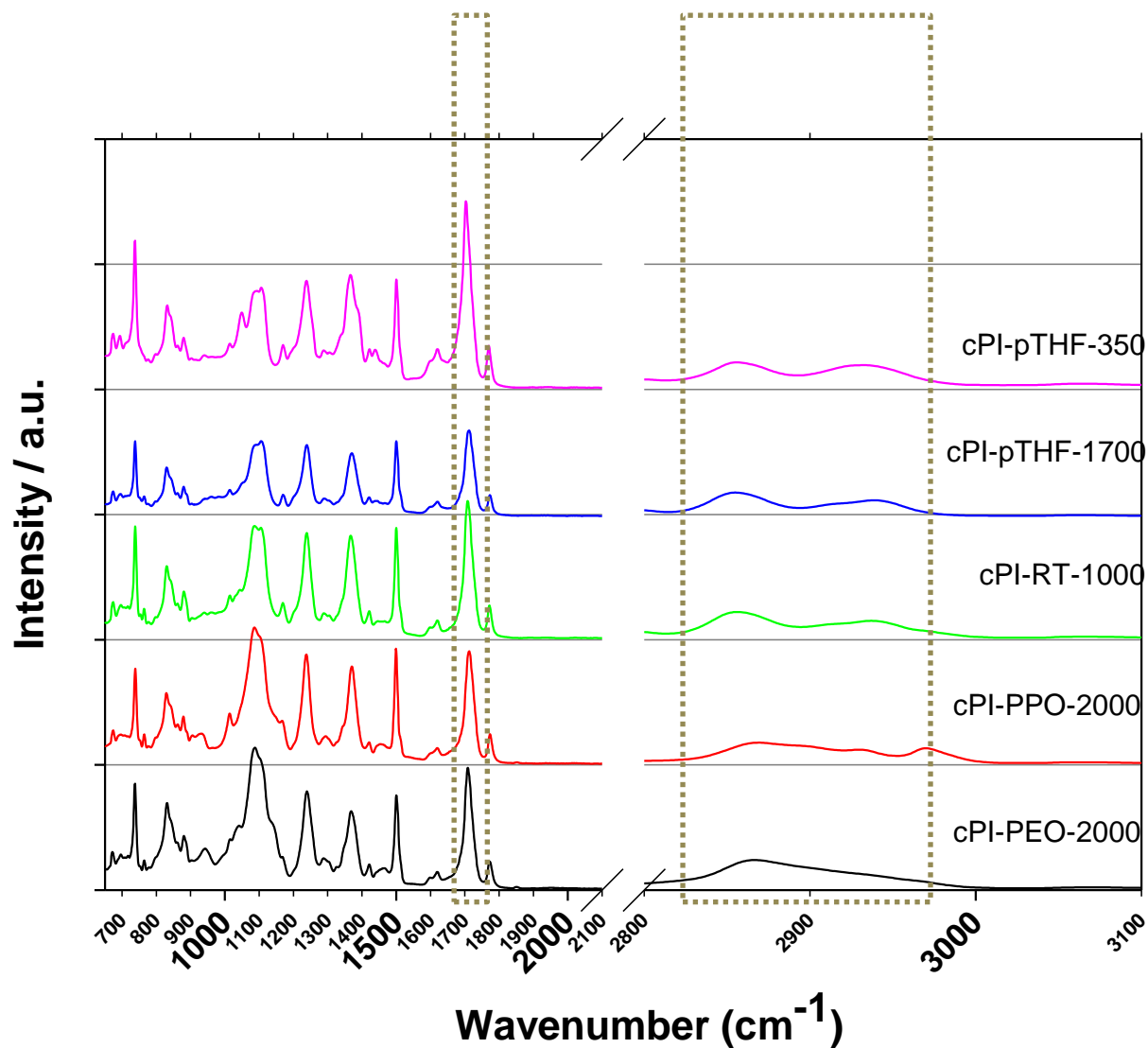


Figure 2.-ATR-FTIR Spectra of copoly(ether-imide)s .

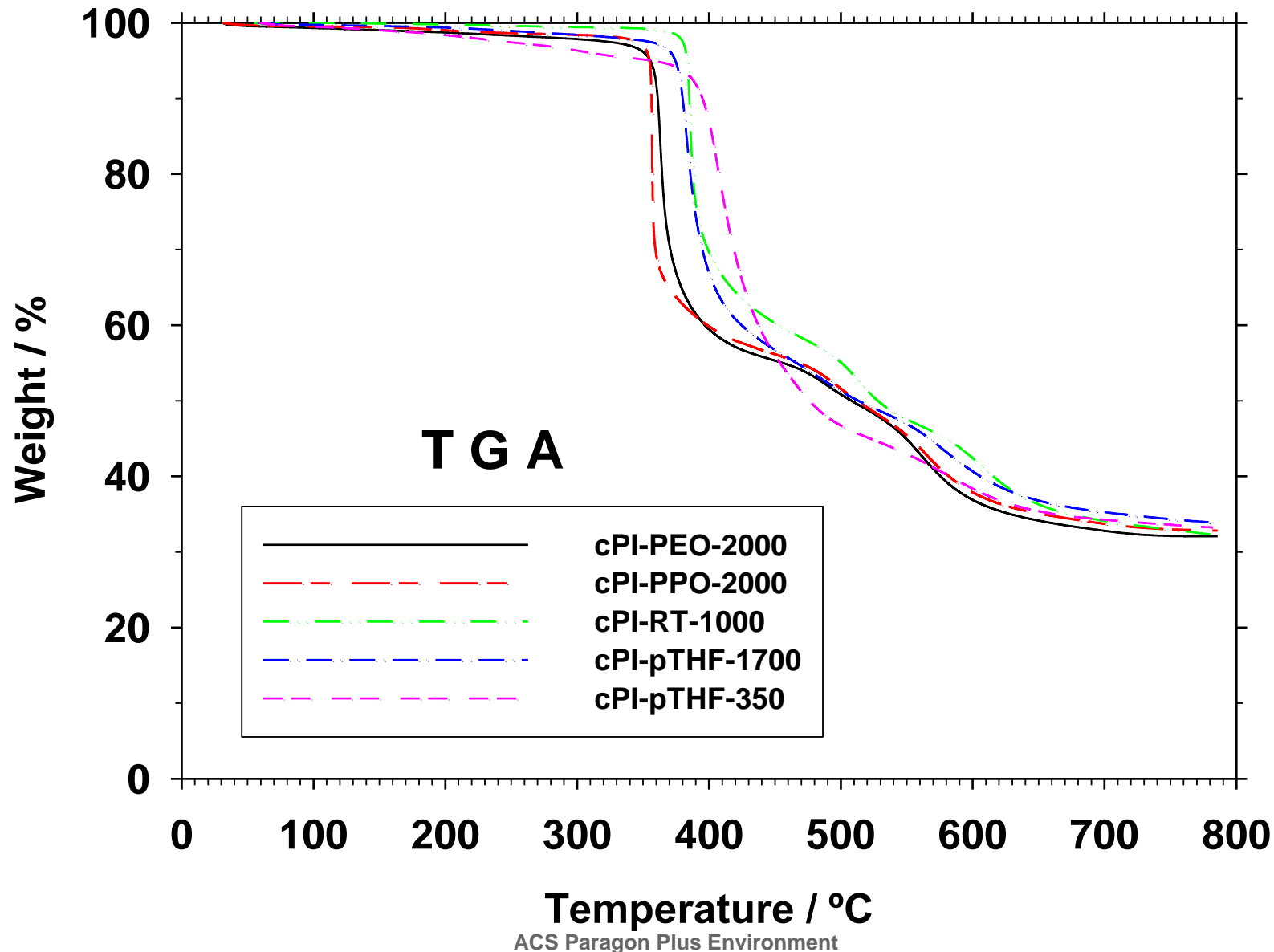


Figure 3. TGA curves in dynamic conditions of copolymers having different aliphatic diamines.

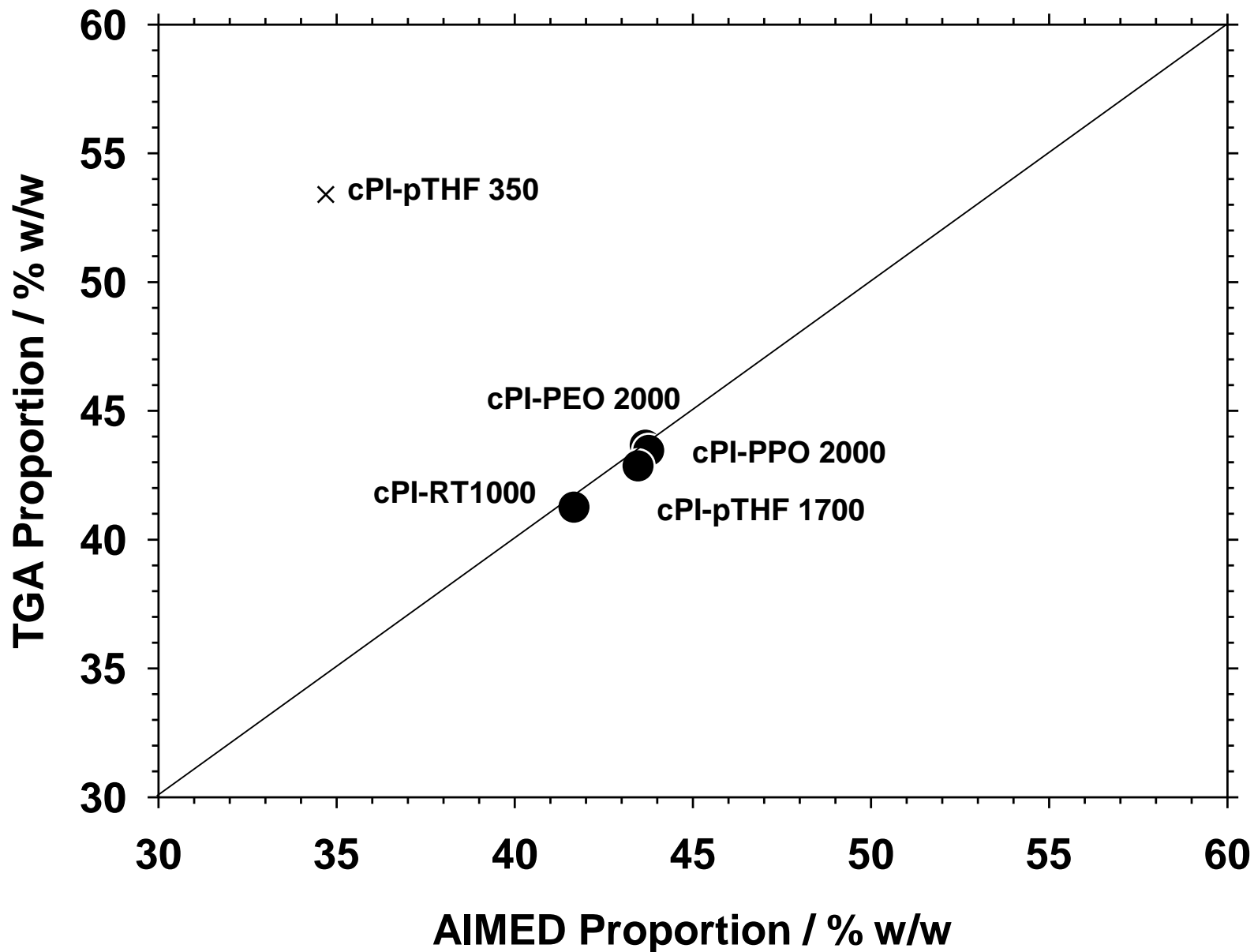


Figure 4. Aliphatic mass losses obtained from TGA versus the corresponding mass proportions according to the manufacture procedure

1
2
3
4
5
6
7
8
9
10
11
12
13
14
15
16
17
18
19
20
21
22
23
24
25
26
27
28
29
30
31
32
33
34
35
36
37
38
39
40
41
42

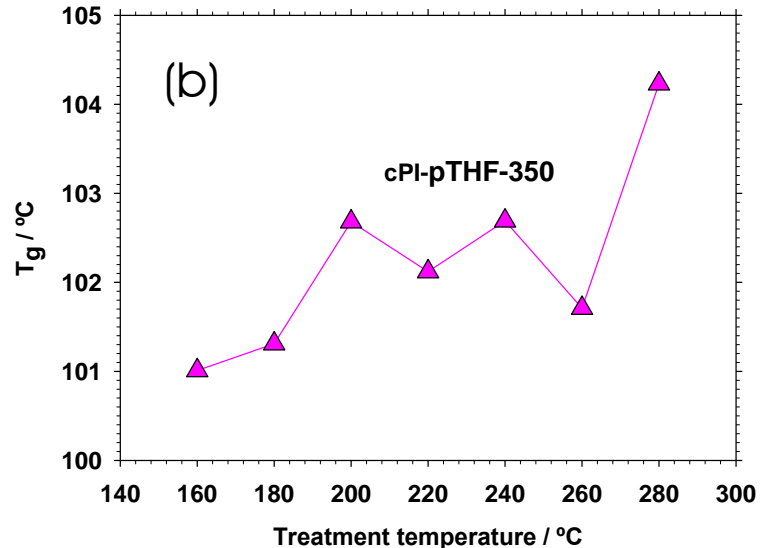
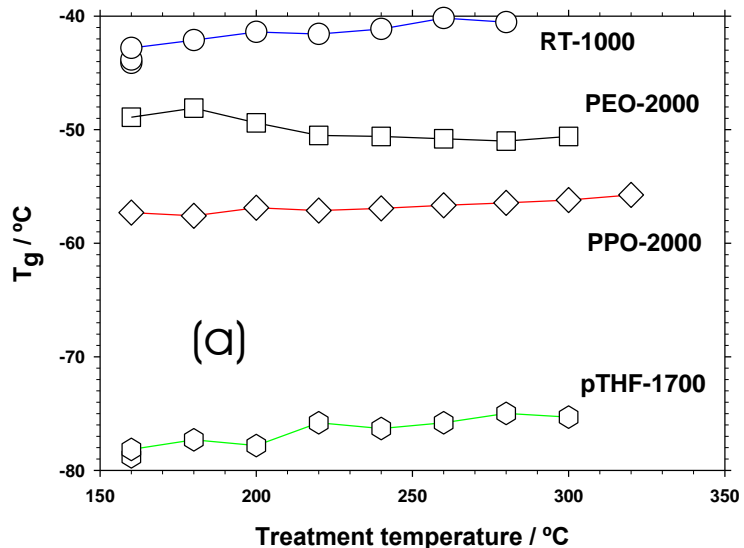


Figure 5.- a) T_g of the aliphatic part of copolymers as a function of the thermal treatment. For the sake of readability, T_g of the aliphatic part of cPI-THF-350 is shown in Figure 5(b).

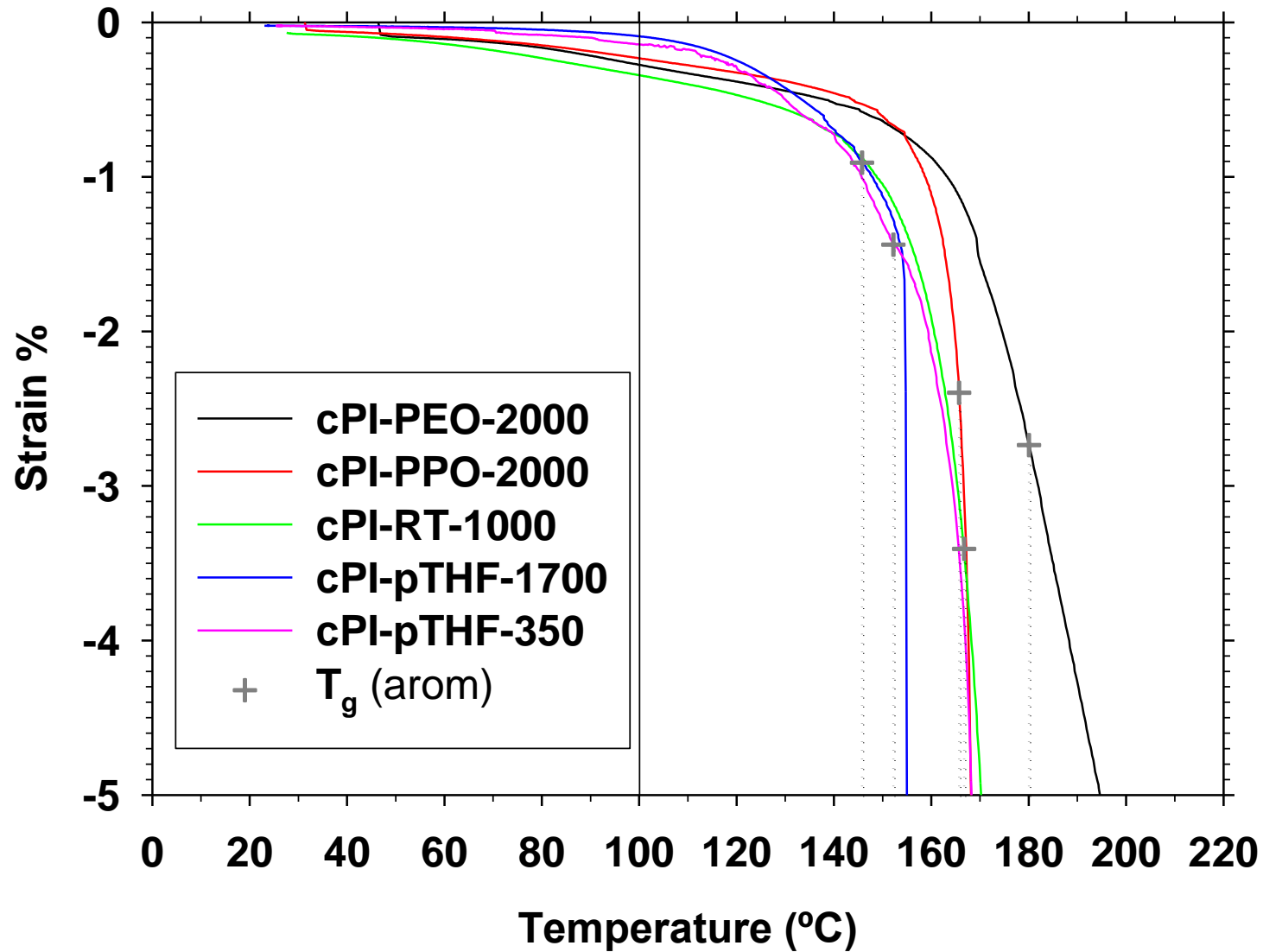


Figure 6.-TMA curves of copolyimides. Crosses correspond to the T_g for the aromatic segment.

These polymer films were treated at 160 °C

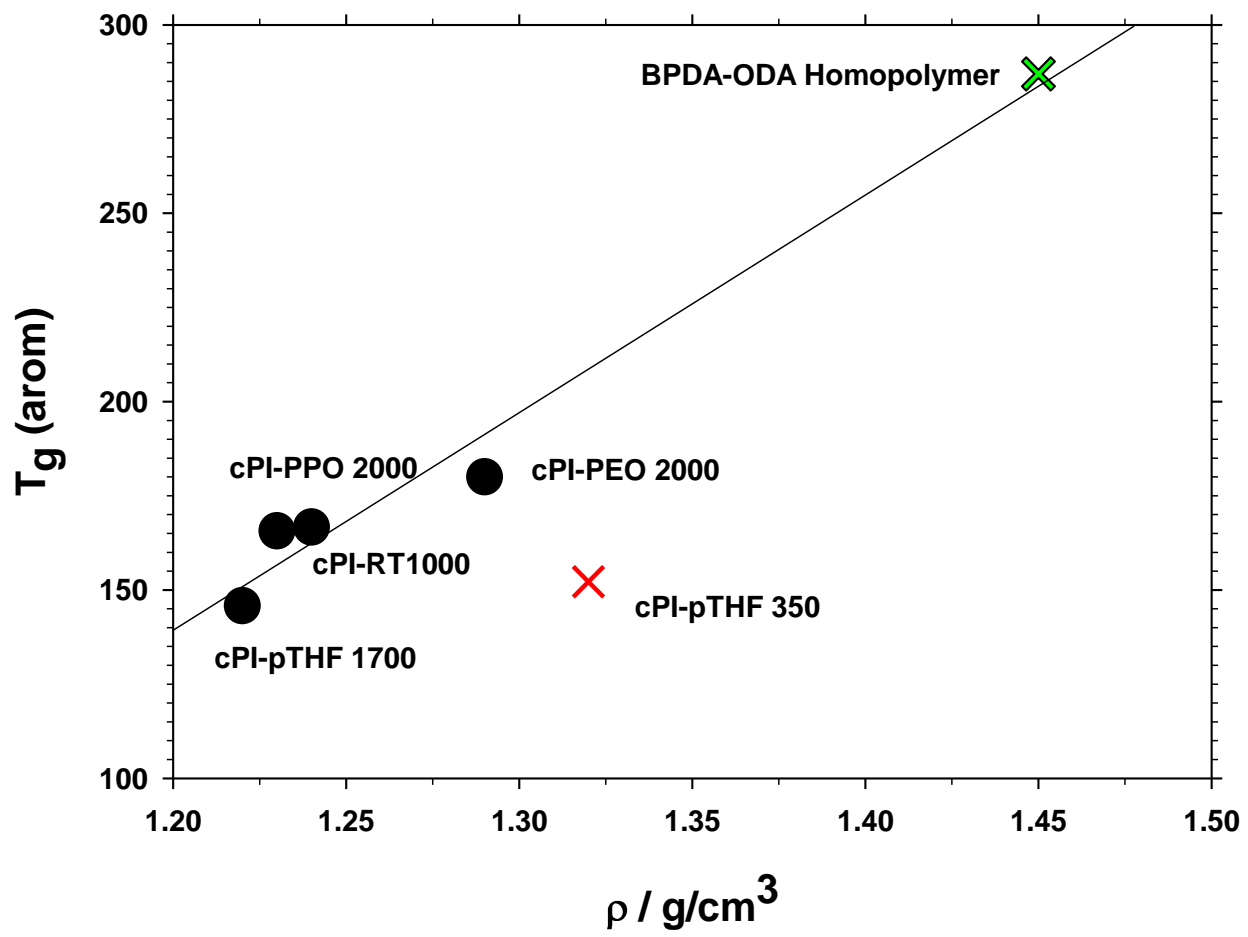


Figure 7. T_g of the aromatic parts of copolymers (as shown in Figure 6) versus the density of these copolymers. Density and T_g for BPDA-ODA homopolymer are shown in the graph. Polymer films were treated at 160 °C.

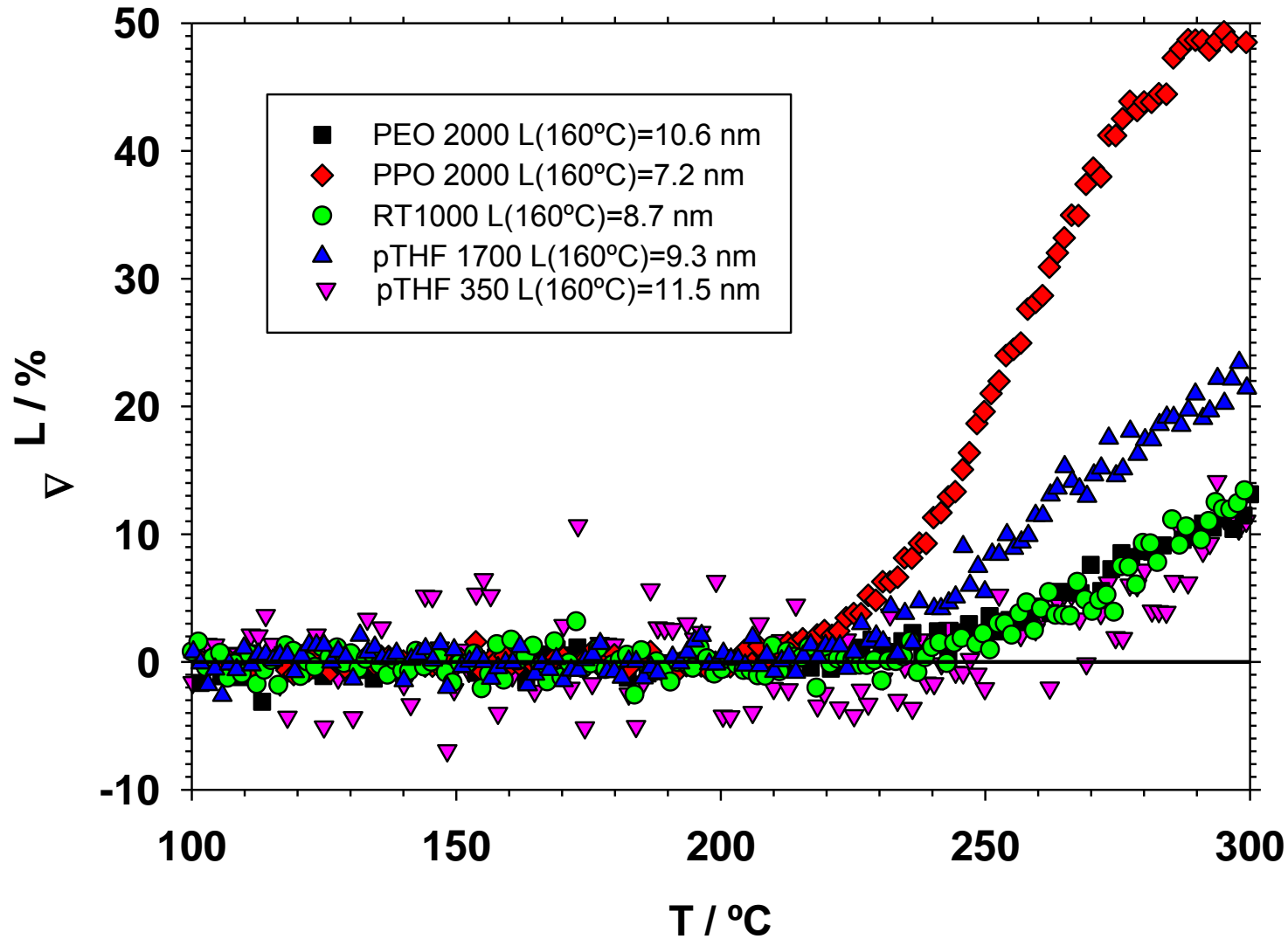


Figure 8. ΔL of copolymers as a function of treatment temperature. The characteristic length for the treatment at 160 °C is shown in the legend. Polymer films were treated at 160 °C.

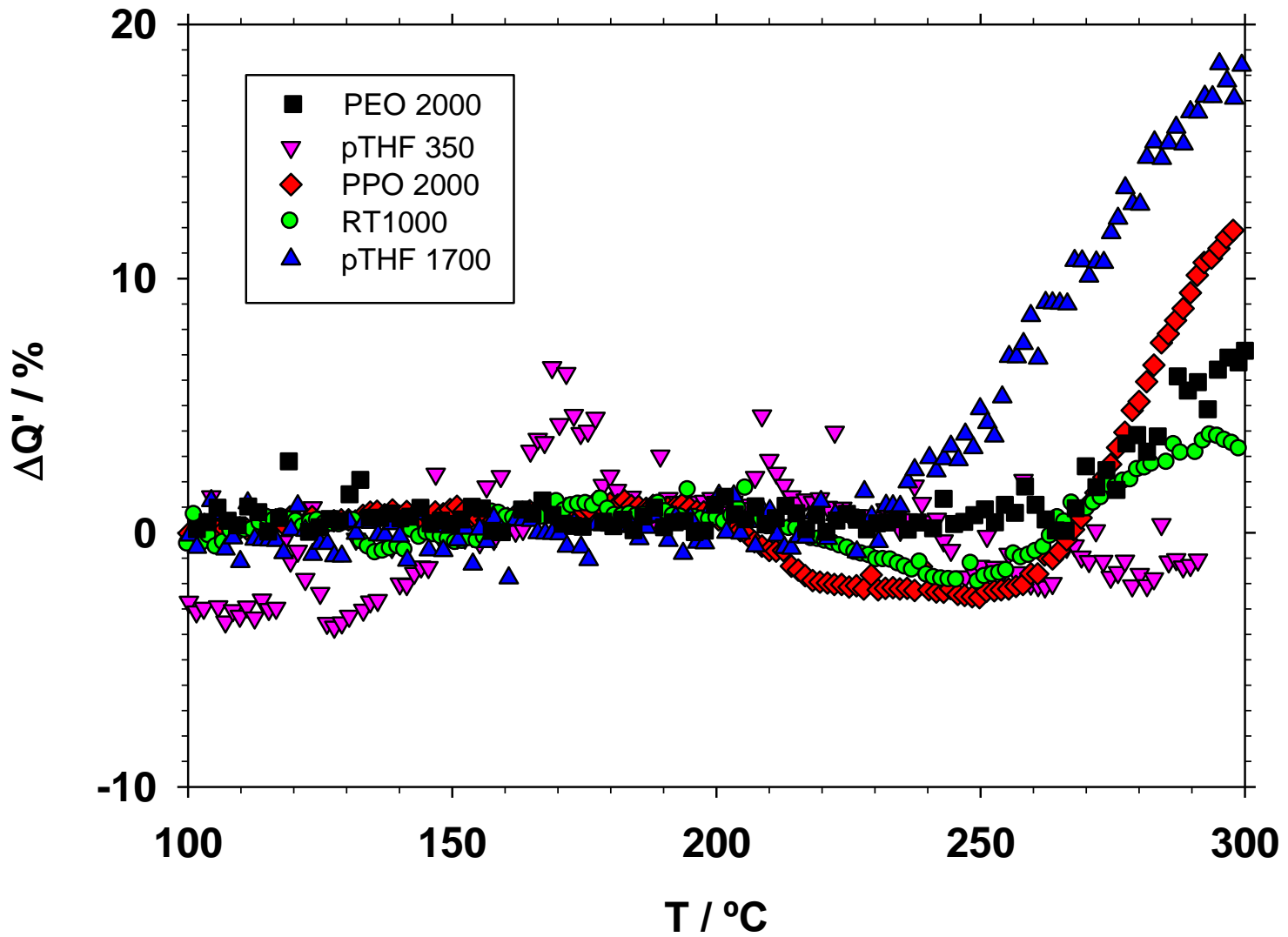


Figure 9. $\Delta Q'$ of copolymers as a function of temperature. Polymer films were treated at 160 °C.

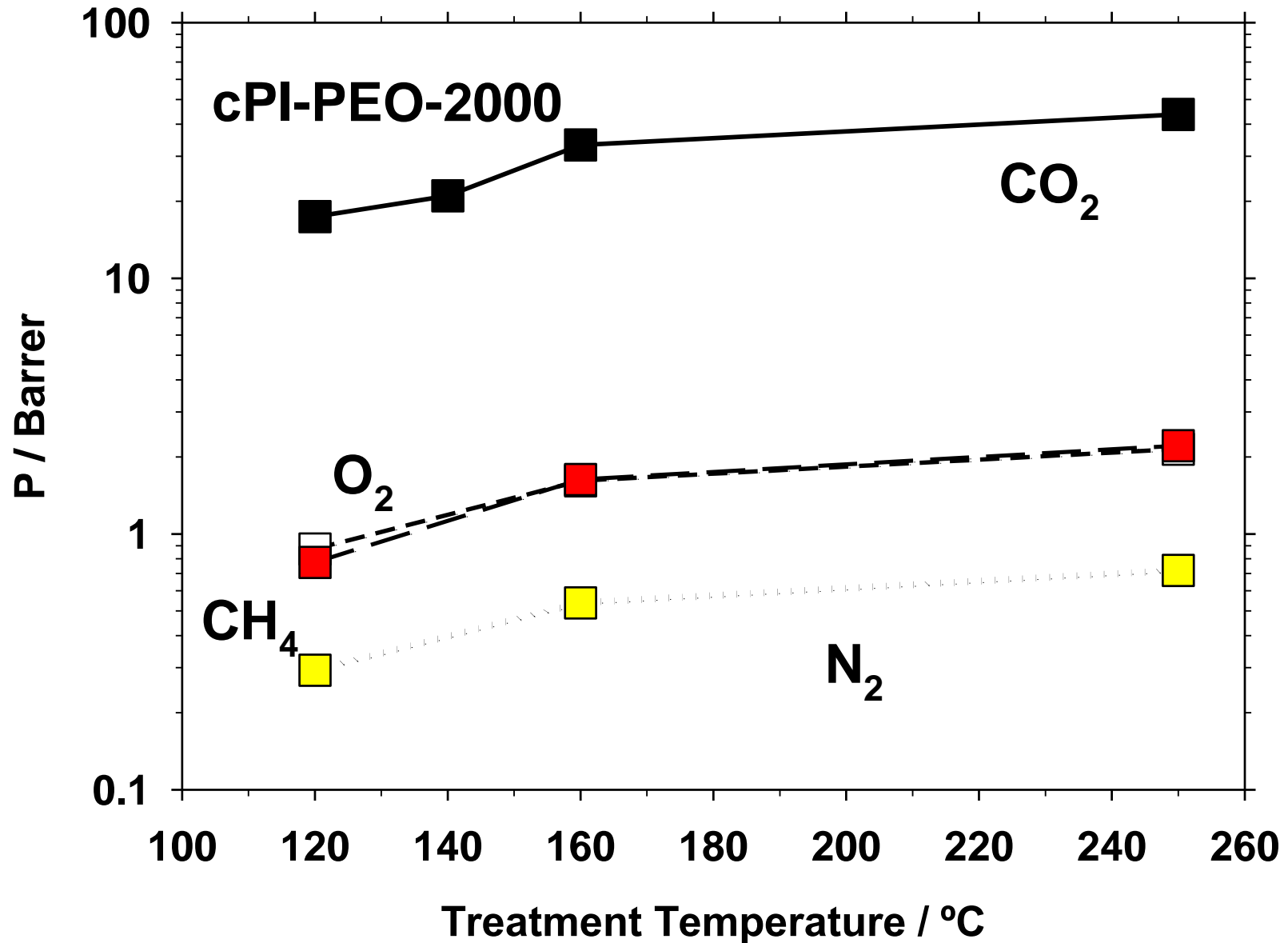


Figure 10. Permeability of the different gases studied as a function of the temperature of treatment for cPI-PEO-2000 copolymer.

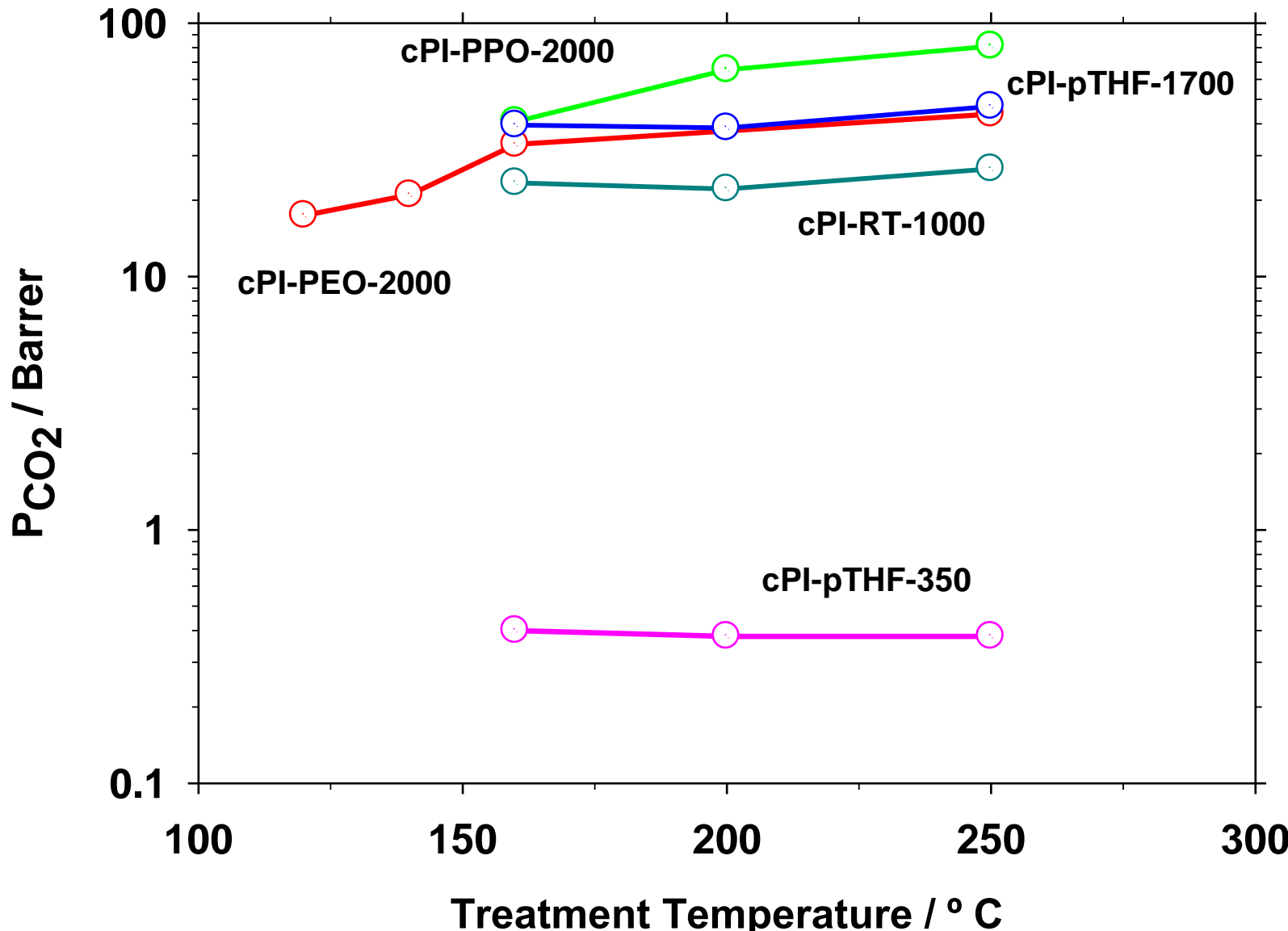


Figure 11. Permeability of CO₂ for different copolyimides as a function of the temperature of treatment.

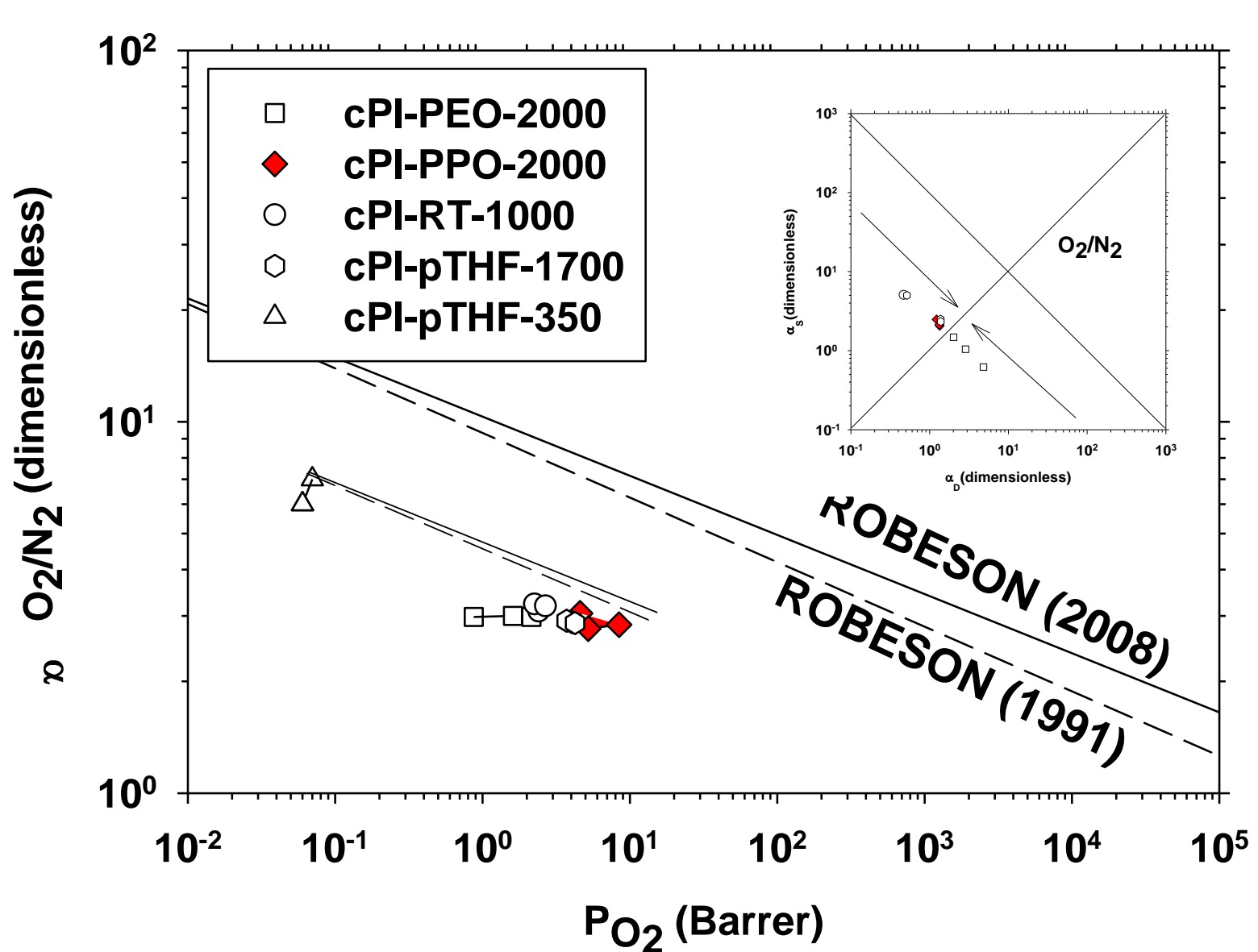


Figure 12. Robeson plot of copolymers for the O_2/N_2 gas pair. The insert shows the corresponding solubility and diffusivity selectivities.

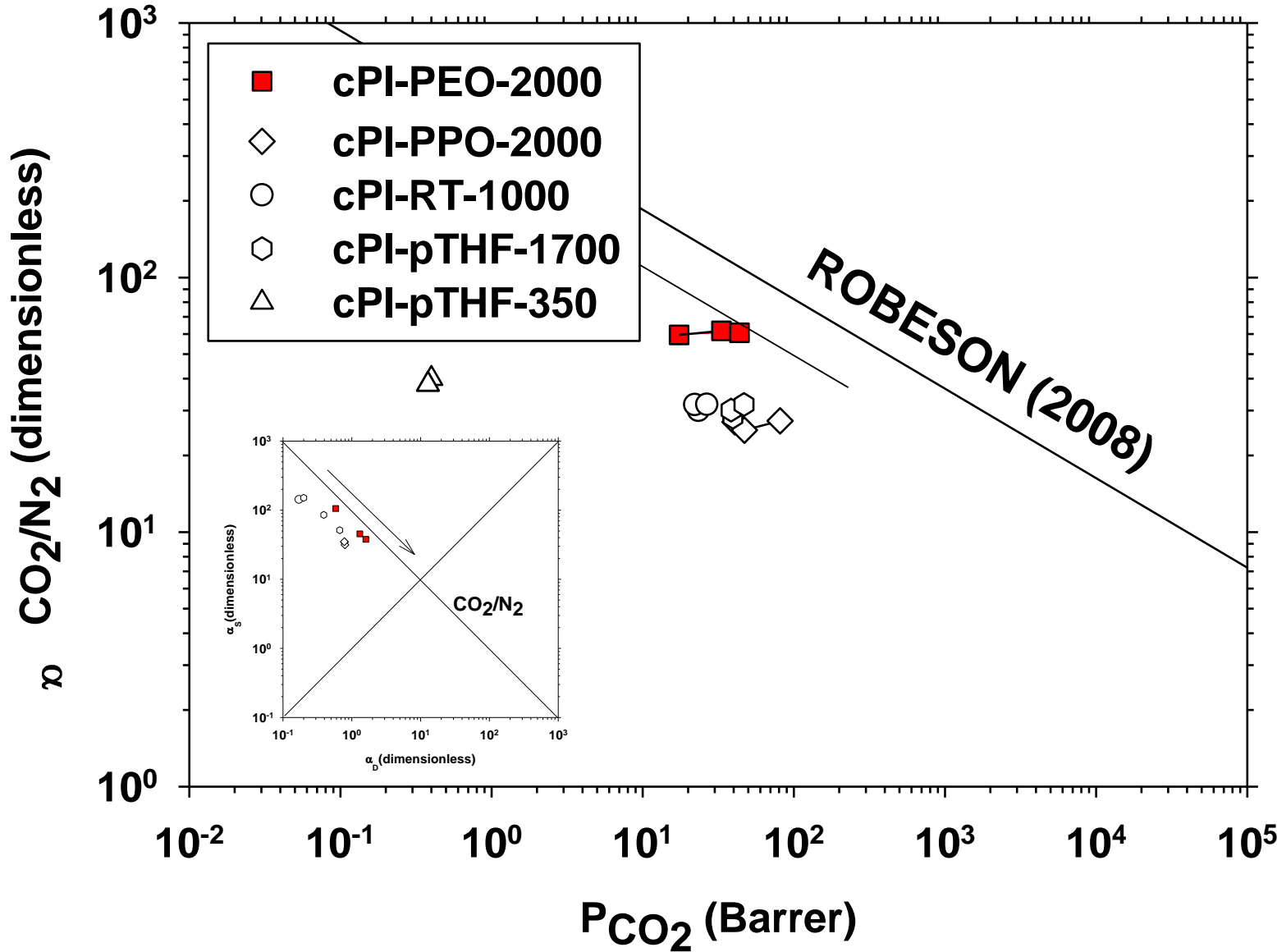


Figure 13. Robeson plot of copolymers for the CO_2/N_2 gas pair. The insert shows the corresponding solubility and diffusivity selectivities.

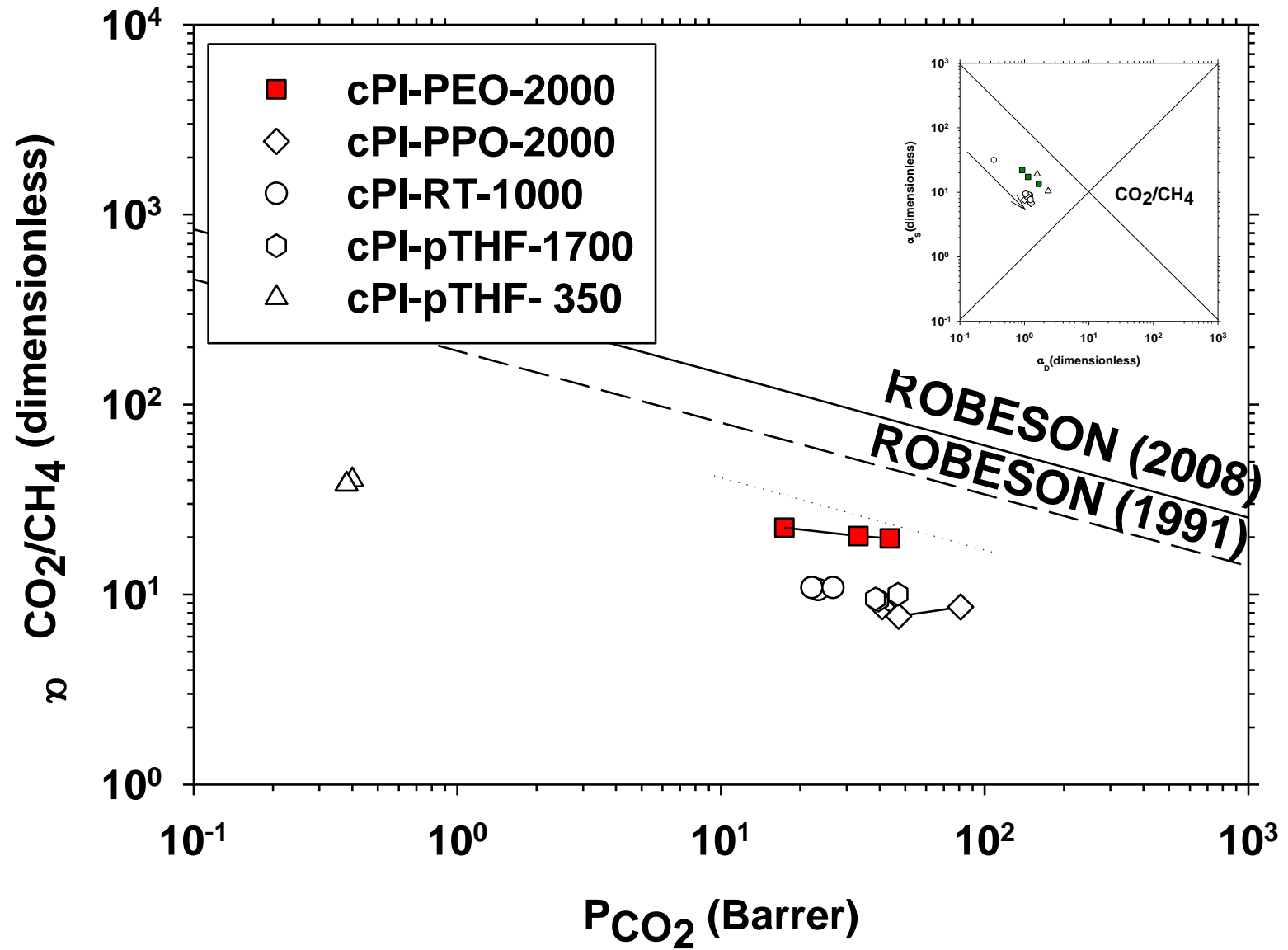
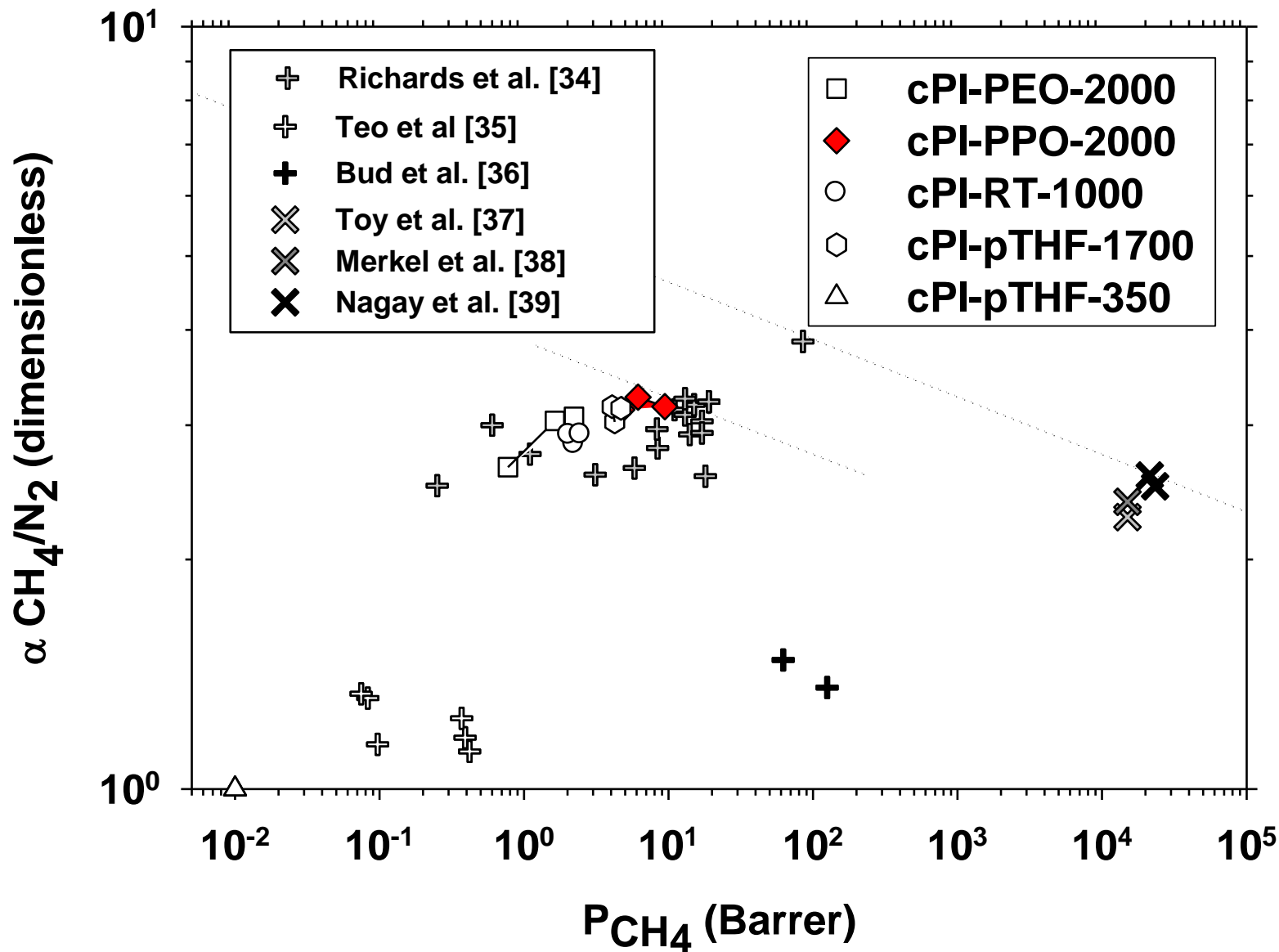
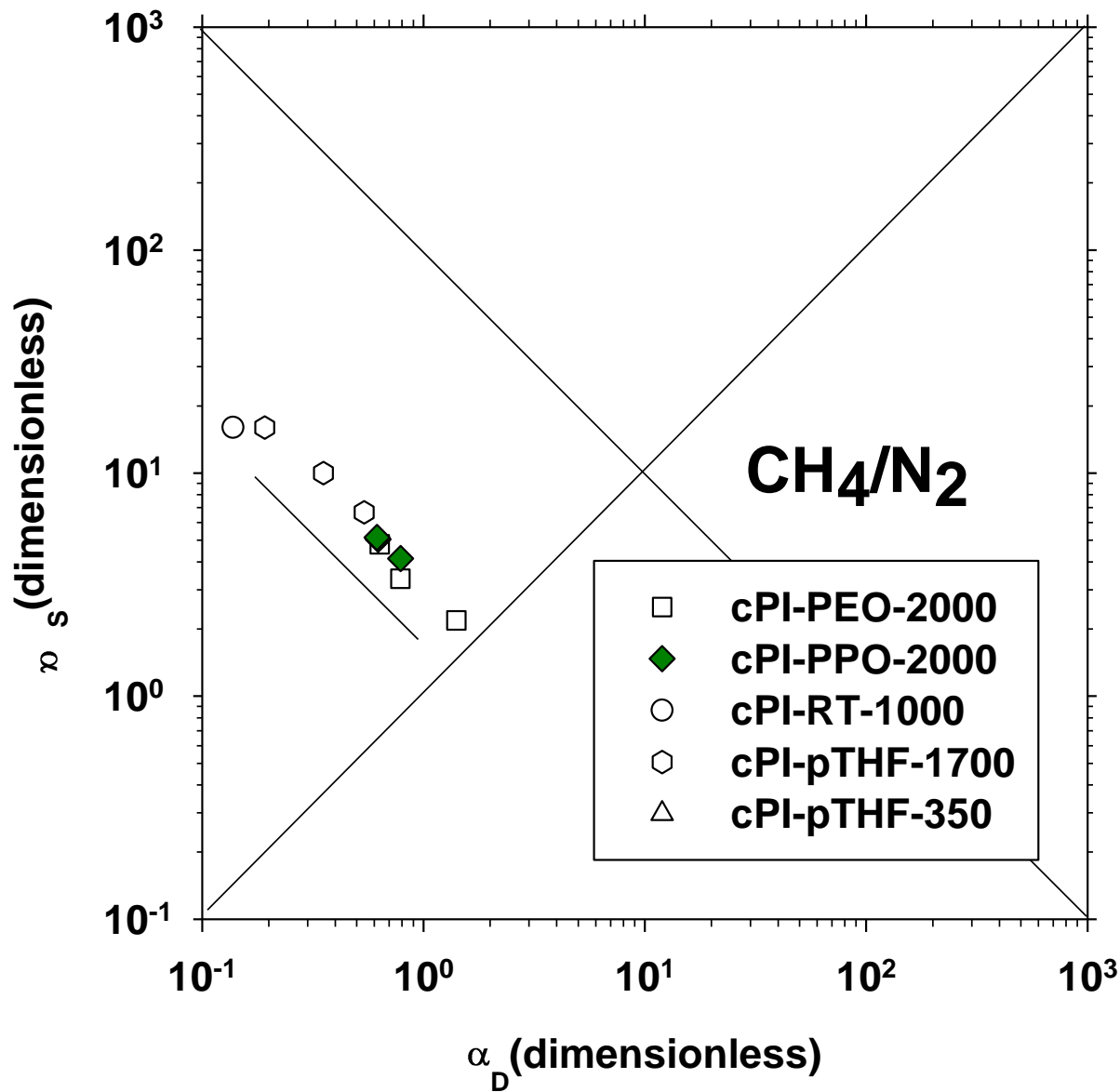


Figure 14. Robeson plot of copolymers for the CO₂/CH₄ gas pair. The insert shows the corresponding solubility and diffusivity selectivities.



ACS Paragon Plus Environment

Figure 15. Robeson plot of copolymers for the CH_4/N_2 gas pair.

Figure 16. Solubility and diffusivity selectivities of copolymers for the CH₄/N₂ gas pair.

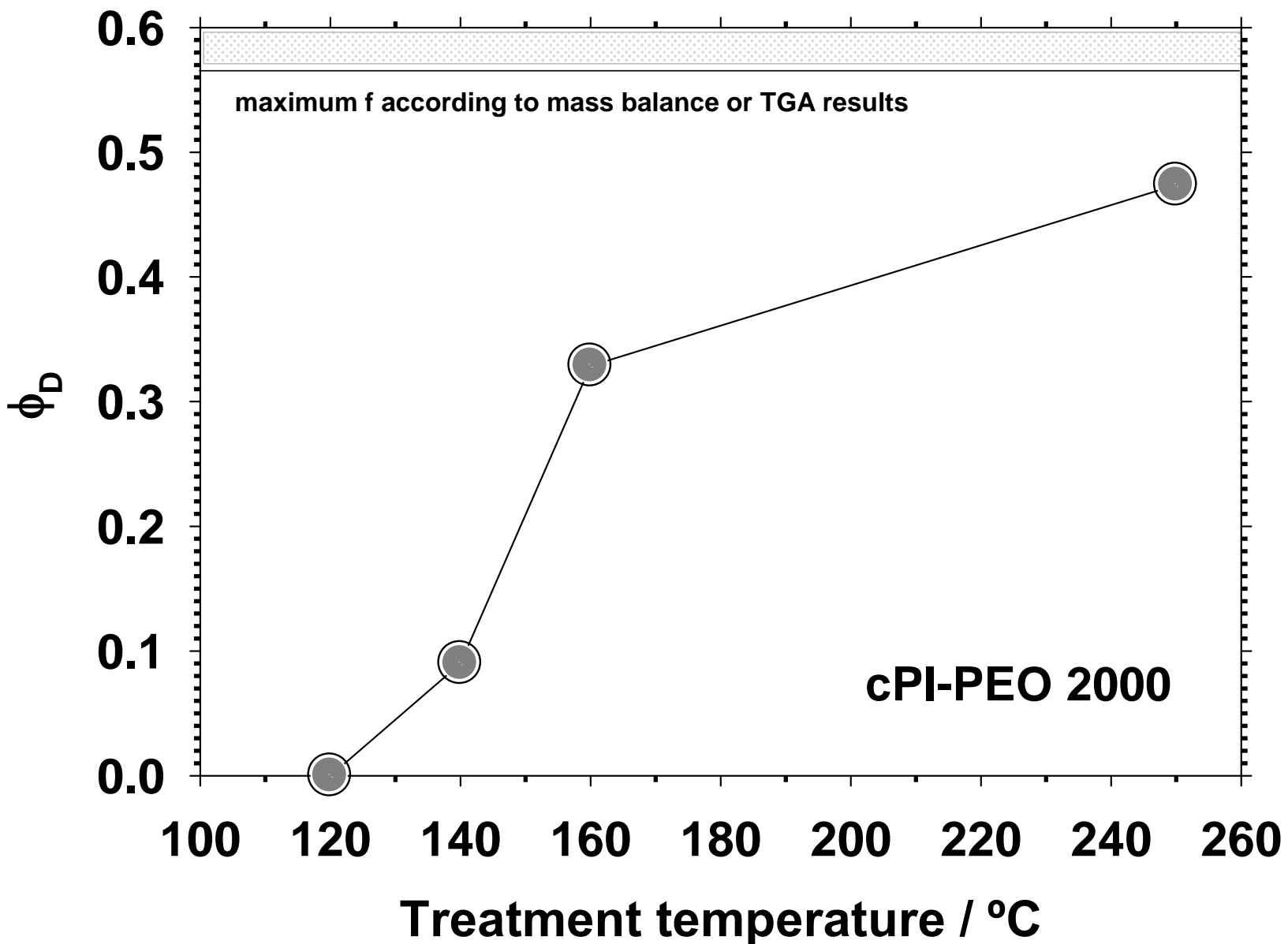


Figure 17. Volume fraction of phase segregated PEO for cPI-PEO-2000 as a function of the treatment temperature.